Reviewer(s)' Comments to Author:

Reviewer: 1

Comments:

General Comment

Gaseous hydrochloric and hydrobromic acid play important roles in tropospheric physicochemical processes, however, the atmospheric gaseous HCl and HBr in urban environments, are much less studied. This manuscript focused on the concurrent measurement of gaseous HCl and HBr by a CI-APi-LTOF mass spectrometer in urban Beijing, China, which is rarely reported before. Strong gaseous HCl and HBr were observed in Beijing where marine sources only have limited influence. Anthropogenic emissions seem to be a more important factor. This study estimates the production of atomic Cl and Br by the reactions of HCl and HBr with OH, which further contribute to atmospheric oxidation capacity. It provides a new insight of halogen chemistry in Chinese megacities and fits the scope and the interest of the journal of ACP. It is well organized and professionally written. Therefore, I recommend this manuscript for publication after minor revisions.

Reply: We are very grateful to the positive comments and helpful suggestions from Reviewer #1, and have carefully revised our manuscript accordingly. A point-to-point response to reviewers' comments, which are repeated in italic, is given below.

Comments:

1. Line 5: In the authors list, it seems to be press error that some affiliations are marked with superscript and the rest ones are with subscript.

Reply: Thanks for pointing it out. We have corrected this typo in our revised manuscript.

2. Line 115: Besides HNO_3, some other strong acids such as gaseous H_2SO_4 can also displace HX from sea-salt particles (Thornton et al., 2010). The authors should also add that information.

Reply: We have added this information to our revised manuscript.

Revised text in the main text (line 112-115):

"It is known that sea-salt particle is a major source of atomic halogens in the marine environment. The chloride (Cl^-) and bromide (Br^-) in the sea-salt particles can be displaced by strong acids (i.e., nitric acid (HNO_3) and sulfuric acid (H_2SO_4)) to release gas-phase hydrogen halides HX (reaction (R1); X = Cl or Br) into the atmosphere (Gard et al., 1998;Thornton et al., 2010)."

3. Line 174 delete the words of "atmospheric Br".

Reply: We have removed the words "atmospheric Br".

Revised text in main text (line 173-176):

"Yet, since the phasing out of leaded gasoline, the long-term atmospheric Br exhibited a continuous decreasing trend for 2 to 3 decades in Germany (Lammel et al., 2002), and a similar situation is expected in Beijing as the usage of leaded gasoline was banned from the years around the 2000s in China (Cai et al., 2017)."

4. Line 178 "Crisp et al. (Crisp et al., 2014) summarized that…" should be revise to "Crisp et al. summarized that…".

Reply: We have revised accordingly.

Revised text in the main text (line 179-184):

"Some limited studies focused on the atmospheric HCl, for example, Crisp et al. (2014) summarized that the concentration of HCl is typically less than 1 ppb over the continental regions and McNamara et al. (2020) measured the concentration of HCl is around 100 ppt from inland sources, while an airborne measurement showed HCl concentrations of around 100 ppt was typically observed over the land area of northeast United States, except near power plant plumes with concentrations over 1 ppb (Crisp et al., 2014;McNamara et al. 2020;Haskins et al., 2018)."

5. To better present the results, I recommend the authors to improve the quality of the figures. Take Figure 6 for example, to better present the comparison, panel C can be divided into two sub-panels. The sizes of the panels of Figure 4, Figure S9 and S10 should be the same.

Reply: Thank you for your advice. These figures have already been improved accordingly. Figure S9 has been moved to the revised main text as Figure 5. The original Figure 6 and Figure S10 were changed to Figure 7 in the revised main text and Figure S9 in revised SI, respectively. To make it easier to view, these revised figures were attached below.

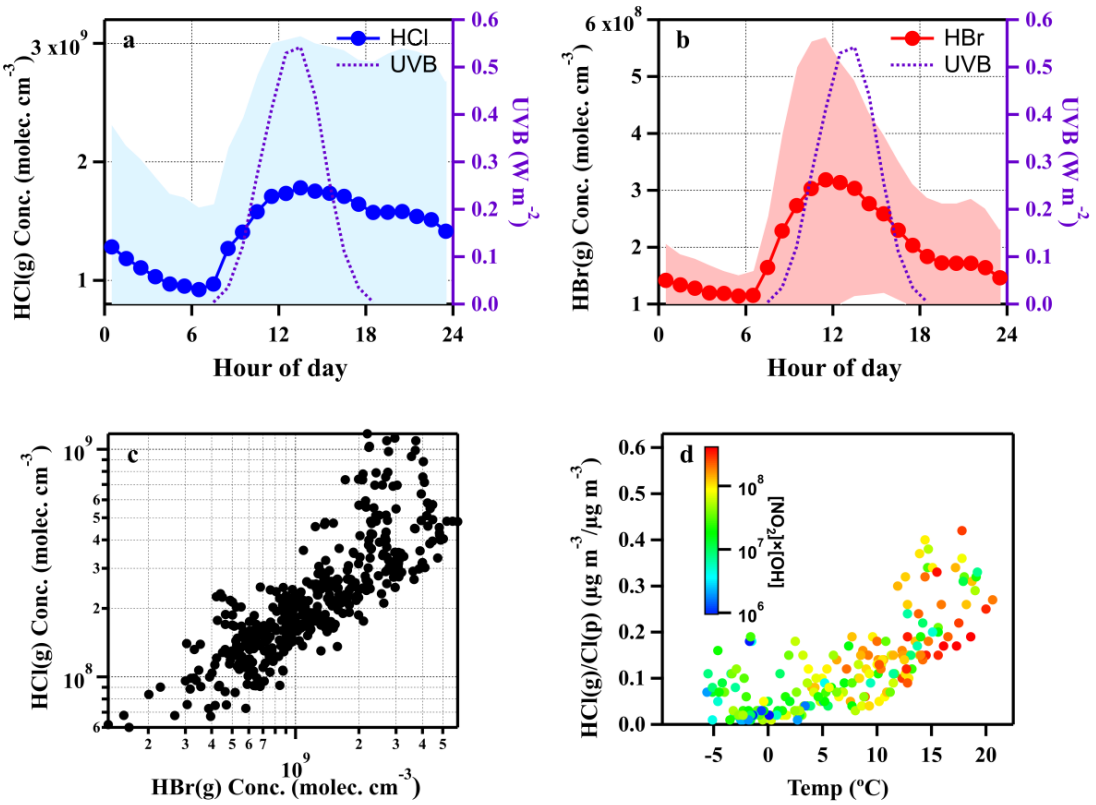

Figure R1 (Figure 4 in the revised main text). Diurnal variations of UVB intensities, HCl and HBr concentrations (averaged values ± one standard deviation) (**a** and **b**) and the correlation between HCl and HBr (**c**). In panel c, the data points are hourly averaged ones during daytime (8:00-17:00). Temperature dependence of gas to particle partitioning ratios of mass concentration of chloride, colour-coded by $[NO_2]$*[OH] which was indicated as the abundance of HNO_3 (**d**). All snowy and rainy days during the sampling period were excluded.

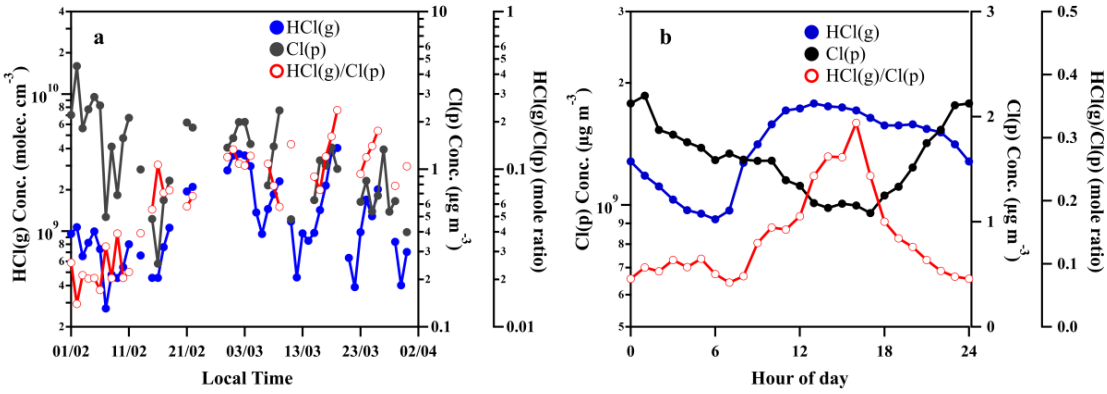

Figure R2 (Figure 5 in the revised main text). Time profile of daily averaged concentration of particulate chloride (Cl(p)) measured by ACSM, gaseous HCl (HCl(g)) measured by CI-APi-LTOF and the mole ratio of HCl(g)/Cl(p) (**a**) and diurnal variation of HCl(g), Cl (p) and HCl(g)/Cl(p) (**b**).

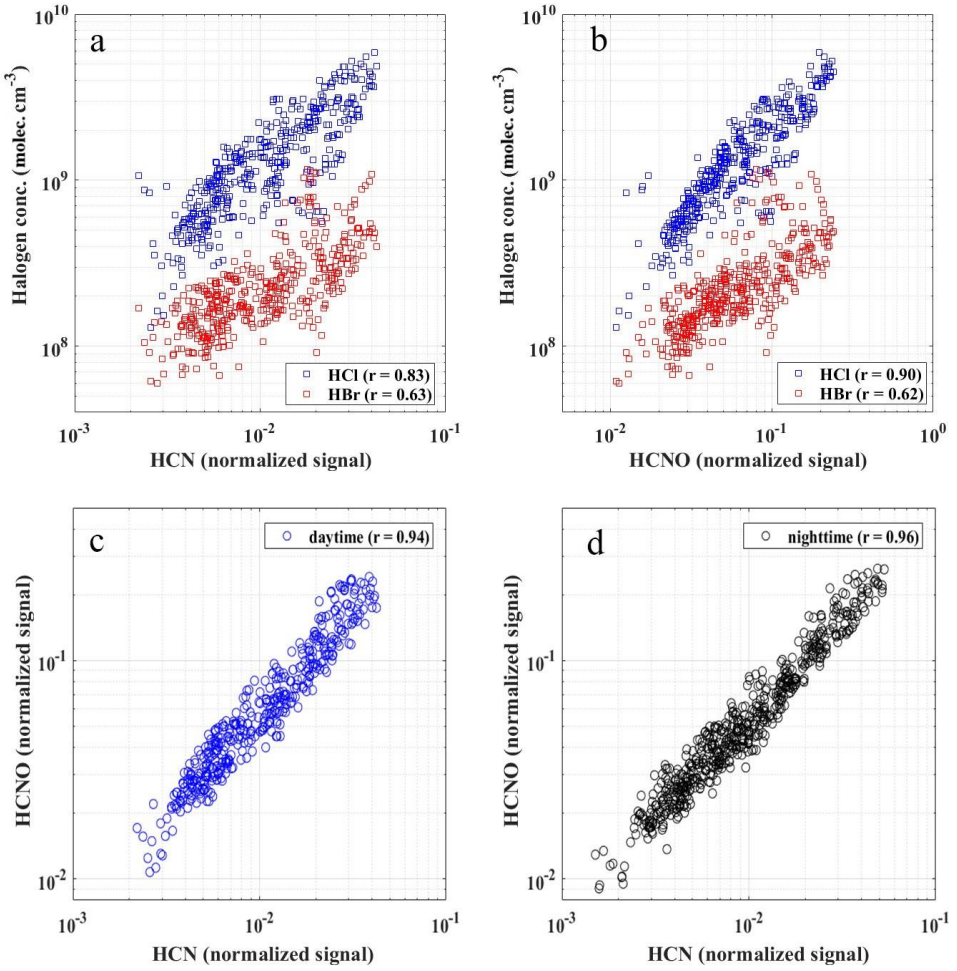

Figure R3 (Figure 7 in the revised main text). The relationship of HCl and HBr concentrations with HCN (**a**) and HCNO (**b**) during the daytime (08:00-17:00) and the correlations between HCN and HCNO during both daytime (08:00-17:00) (**c**) and nighttime (18:00-07:00 the next day) (**d**). The data points are hourly averaged ones.

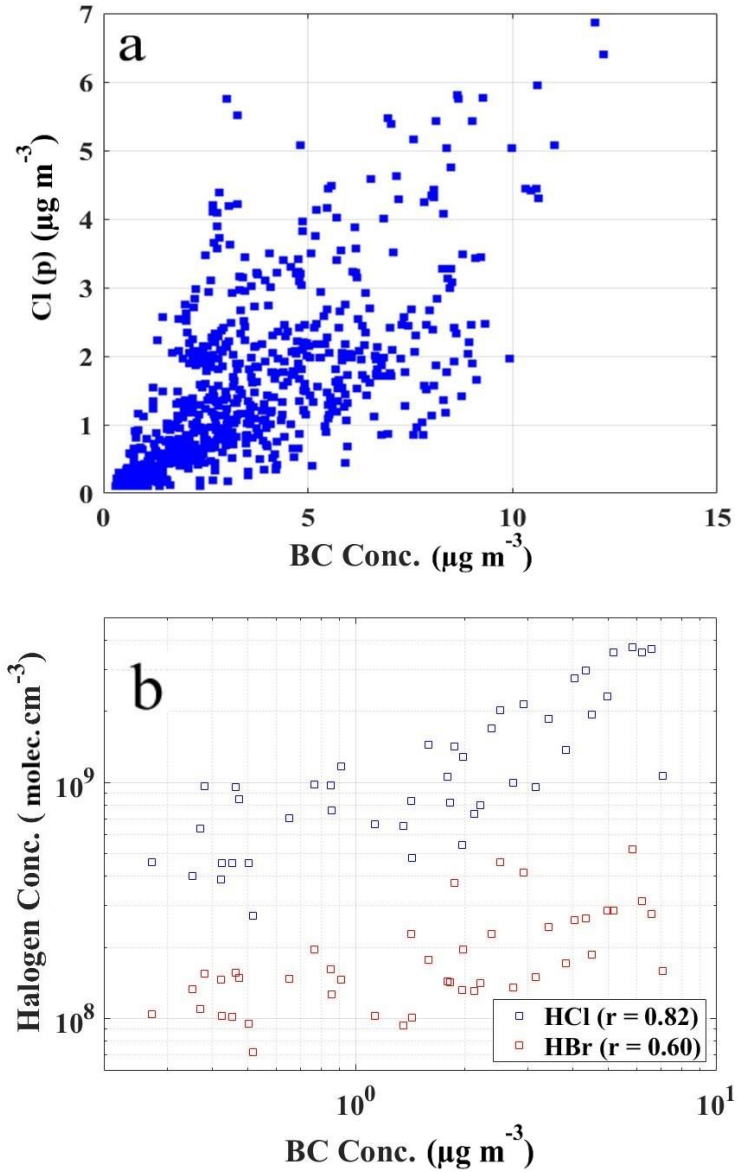

Figure R4 (Figure S10 in the revised SI). The correlation (r = 0.67) between hourly mean mass concentrations of particulate Cl (Cl(p)) and black carbon (BC) (**a**); correlations between daily mean concentrations of HCl (r = 0.82), HBr (r = 0.60) and BC during observation periods from 1 February to 31 March, 2019 (**b**).

6. In the manuscript, to compare the concentrations of HCl and HBr between Beijing, China in this study and other locations from previous ones (Lee et al., 2018; Simpson et al., 2015), it is better to also include the unit of mixing ratios (i.e., ppt) beside number concentrations (# cm^{-3}) in the measurement.

Reply: We have included the mixing ratios as ppt to the text.

Revised text in the main text (line 52-54):

"We observed significant HCl and HBr concentrations ranged from a minimum value at 1×10^8

molecules cm^{-3} (4 ppt) and 4×10^7 molecules cm^{-3} (1 ppt) up to 6×10^9 molecules cm^{-3} (222 ppt) and 1×10^9 molecules cm^{-3} (37 ppt), respectively."

Revised text in the main text (line 302-304):

"The mean concentrations of HCl and HBr are 1×10^9 molecules cm^{-3} (37 ppt) and 2×10^8 molecules cm^{-3} (7 ppt), respectively. The maximum concentrations reach up to 6×10^9 molecules cm^{-3} (222 ppt) for HCl, and 1×10^9 molecules cm^{-3} (37 ppt) for HBr during the daytime."

7. How do HCl and HBr behave on clean days and polluted days? are their concentrations higher during polluted days?

Reply: HCl and HBr have different behaviors between clean days and polluted days during our observation period. HCl and HBr are more abundant on haze days (daily mean $PM_{2.5} \geq 75$ ug/m^3) than that on clean days (daily mean $PM_{2.5} < 75$ ug/m^3). The detail has been added in "3.3 halogen-atom productions." Please also refer to the reply below for Comment 8.

8. The title of "3.3 halogens atom production" should be "3.3 halogens' atom productions" or "3.3 halogen-atom productions". Besides, this part is interesting and important. Can the authors expend this part a bit to better elucidate the potential applications of the results from the measurement?

Reply: The title "3.3 halogens atom production." has been changed to "3.3 halogen-atom productions.".

Also, this section has been expanded accordingly (Line 414-419):

"The average HCl and HBr concentrations were observed to be higher during the polluted days (daily mean $PM_{2.5} \geq 75$ μg/m^3), which is about 2-3 times higher than the clean days (daily mean $PM_{2.5} < 75$ μg/m^3), as shown in Figure 8b. Consequently, the radical production rate also showed a difference between clean and polluted days (Figure 8d). The daily mean value of P_{Cl}. (up to 8×10^3 molecules cm^{-3} s^{-1}) and P_{Br}. (2×10^4 molecules cm^{-3} s^{-1}) in polluted days were both higher than that of clean days by up to 2 times. This hints that the roles of HCl and HBr may be more significant in polluted environments."

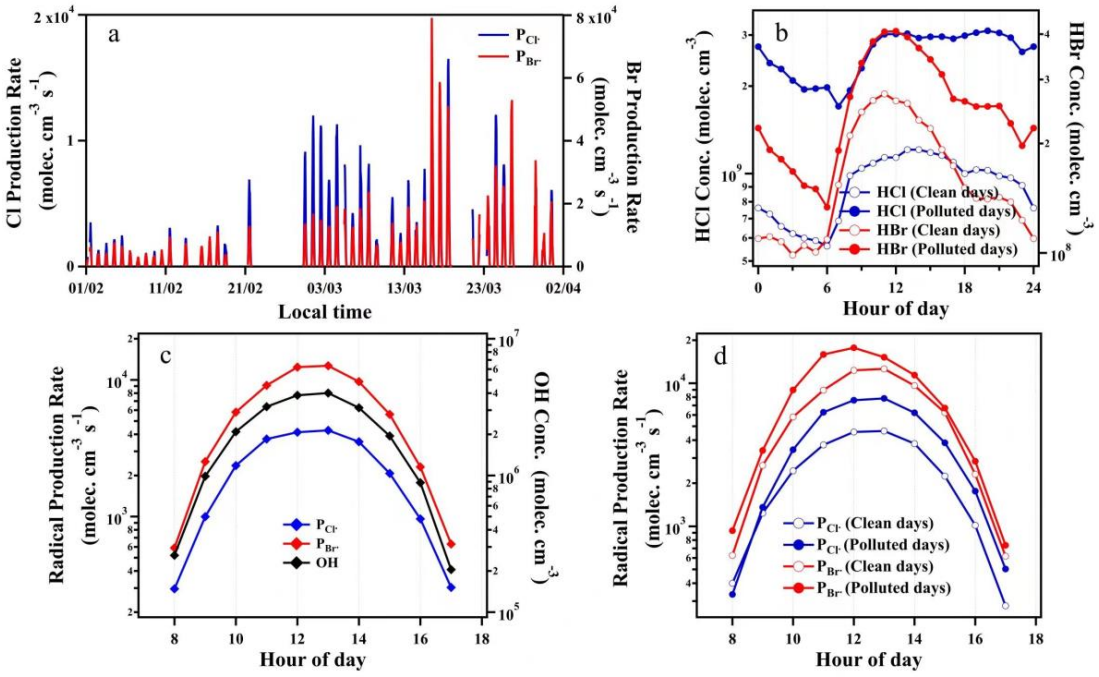

Figure R5 (Figure 8 in the revised main text). Time series of calculated production rates of Cl and Br radicals during the observation period (**a**); diurnal variations of HCl and HBr concentrations in clean and polluted days (**b**); diurnal variations of production rates of Cl and Br radicals, together with calculated OH radical concentrations (**c**) and production rates of Cl and Br radicals in clean and polluted days (**d**). The clean and polluted days were classified as daily $PM_{2.5} < 75$ μg/m^3 and $PM_{2.5} \geq 75$ μg/m^3, respectively. The data points are in the hourly-average interval and measured during observation periods from 1 February to 31 March 2019.

9. In SI, a good correlation was observed between measured J_{NO2} and modelled J_{NO2} (Figure S11). Please add the brief description of the model that used.

Reply: In this study, unfortunately, direct measurement of J_{NO2} is not available during our observation periods. The photolysis rate constants of NO_2 (J_{NO2}) were calculated according to the solar zenith angle and the location using a box model (FACSIMILE 4) (Liu et al., 2020). Then, the output (modelled J_{NO2}) was compared to the measured J_{NO2} (by using NO_2 photolysis sensor (J_{NO2}, Metcon)) for the period when J_{NO2} measurements were available, as shown in Figure S10, to ensure that the modelled J_{NO2} is relevant. We have added the brief description of the model into the SI Section S8 "The calculations of OH concentration and production rate of atomic Cl and Br".

Revised text in SI (line 365-368):

"Photolysis rate constants of NO_2 (J_{NO2}) were calculated according to the solar zenith angle and the location using a box model (FACSIMILE 4) (Liu et al., 2020). Using another dataset collected from 21 May to 10 June 2019, a good correlation (r=0.97) between calculated and measured J_{NO2} confirmed the validation of our calculated J_{NO2} (Figure S11a).

References:

Liu, Y., Zhang, Y., Lian, C., Yan, C., Feng, Z., Zheng, F., Fan, X., Chen, Y., Wang, W., Chu, B., Wang, Y., Cai, J., Du, W., Daellenbach, K. R., Kangasluoma, J., Bianchi, F., Kujansuu, J., Petäjä, T., Wang, X., Hu, B., Wang, Y., Ge, M., He, H., and Kulmala, M.: The promotion effect of nitrous acid on aerosol formation in wintertime in Beijing: the possible contribution of traffic-related emissions, Atmos. Chem. Phys., 20, 13023-13040, 10.5194/acp-20-13023-2020, 2020.

Reviewer(s)' Comments to Author:

Reviewer: 2

Comments:

General Comment

Fan et al present measurements of HCl and HBr in Beijing during winter. This is a unique dataset for which publication is worthwhile. My comments below mainly focus on clarifications and reporting uncertainties.

Reply: We are very grateful for the positive comments and helpful suggestions. And we have carefully revised our manuscript accordingly. A point-to-point response to reviewers' comments (in italic), is given below.

Major Comments:

1. Measurement uncertainties need to be reported and shown throughout (including in main text and in figures), with the proper significant figures reported reflecting this uncertainty. In particular, often HBr values are presented quantitatively and with more certainty (over-reported in terms of significant figures) than is appropriate when the methods (Line 259) state that HBr concentrations should be treated as semi-quantitative (fix word in text); for example, HBr is reported with 2 significant figures even at the single ppt level on Line 52 in the abstract, giving the impression of much greater certainty in this number. When error is reported, it should be with 1 significant figure (unlike on Line 286, where it should also be clarified that this is the standard deviation, I believe?).

Reply: Thanks for the suggestion. We agree with the reviewer that reporting the uncertainty and showing proper significant figures are important. We added the information of the measurement uncertainty calculations as suggested in SI (Section S5. Calibration factor and Uncertainty estimation) line 261-282:

The uncertainties of HCl and HBr measurement come from two parts: (1) the HCl measurement uncertainties coming from MARGA (δ_{MARGA}) and (2) fitting errors coming from the intercomparison between MARGA and CI-APi-LTOF measurements ($\delta_{MARGA\text{-}LTOF}$). The total uncertainties were calculated with the uncertainties propagation equation shown in Eq. (1). The δ_{MARGA} was obtained from many previous studies and assumed to be 15% (Trebs et al., 2004; Du et al., 2010, 2011; Wang et al., 2013). The $\delta_{MARGA\text{-}LTOF}$ was calculated through a procedure implemented in MATLAB (Mathworks, Inc.) from the fitting errors between HCl concentrations measured by MARGA and normalized HCl signals from CI-APi-LTOF in the intercomparison from the period of 2 to 6 September 2019 (shown in Table R1 and Figure S8). $\delta_{MARGA\text{-}LTOF}$ varied from 11% to 24% according to the fitting calculations (with 95% confidence bounds). To be more conservative, $\delta_{MARGA\text{-}LTOF}$ of 0.24 was applied into Eq. (1) to calculate the

total uncertainty (δ). Therefore, the total uncertainty of ± 30% was estimated in reporting HCl concentrations. The uncertainties for HBr were assumed to be the same with HCl since it is assumed that HCl and HBr have the same sensitivities for CI-APi-LTOF.

$$\delta = \sqrt{\delta_{MARGA}^2 + \delta_{MARGA-LTOF}^2} = \sqrt{(0.15)^2 + (0.24)^2} = 0.28 \qquad (1)$$

It should be noted that our assumptions of uncertainties could be regarded as a lower limit of HCl and HBr measurement since other potential uncertainty factors (e.g., different sensitivities of HCl and HBr) were not taken into account.

Table R1 (Table S2 in revised SI). Estimated uncertainty factors in HCl quantification.

	Relative uncertainty (δ)
MARGA measurement	0.15
Intercomparison between MARGA and CI-APi-TOF	0.24

Meanwhile, we have added the uncertainty discussion to the main text and revised some statements accordingly to report proper significant figures.

Revised text in the main text:

Line 52-54:

"We observed significant HCl and HBr concentrations ranged from a minimum value at 1×10^8 molecules cm^{-3} (4 ppt) and 4×10^7 molecules cm^{-3} (1 ppt) up to 6×10^9 molecules cm^{-3} (222 ppt) and 1×10^9 molecules cm^{-3} (37 ppt), respectively."

Line 248-253:

"The obtained calibration factor C_{HCl} for HCl is $3 \pm 0.1\times10^{12}$ molecules cm^{-3} (Figure S8b) and the uncertainty of ± 30% (Section S5) was applied to the reported HCl concentrations. Similar to HCl, the same uncertainty was also adopted for HBr mixing ratios. It should be noted that our assumptions lead towards a lower limit estimate of HCl and HBr concentrations, due to other potential uncertainties (e.g., different sensitivities of HCl and HBr) were not taken into account."

Line 302-304:

"The mean concentrations of HCl and HBr are 1×10^9 molecules cm^{-3} (37 ppt) and 2×10^8 molecules cm^{-3} (7 ppt), respectively. The maximum concentrations reach up to 6×10^9 molecules cm^{-3} (222 ppt) for HCl, and 1×10^9 molecules cm^{-3} (37 ppt) for HBr during the daytime."

2. In addition, for improved comparisons to other work and other atmospheric species, it would be helpful for HCl and HBr to be reported as mole ratios, in addition to the units of molec cm^{-3} (also please add "molec" before cm^{-3} throughout for clarity); this can be done in parentheses

following the current units of molec cm^{-3}, for example. Also, I did not see background/blank measurements discussed, and measurement limits of detection need to be reported.

Reply: The concentration unit was revised from "cm^{-3}" to "molecules cm^{-3}" throughout the whole manuscript.

In this study, background/blank measurement was conducted by zero air measurement and the limits of detection (LODs) were defined as 3 times the standard deviation of background signals within a 2 min integration time. Experimental details for background/blank measurement and detection limits estimation were introduced in Section S4 in SI (Section S4 Laboratory experiment of HCl and HBr).

From the background measurement, the normalized background signals of HCl and HBr were found to be 7×10^{-5} and 1×10^{-5}, which represented 1×10^{8} and 1×10^{7} molecules cm^{-3} (i.e., 4 and 0.5 ppt) for HCl and HBr, respectively. We have added the statements of background/blank measurements and LODs in the revised manuscript.

Revised text in Supporting Information (Section S4 Laboratory experiment of HCl and HBr)

Revised text in SI (line 212-219):

"In order to quantitively confirm HCl and HBr can be detected by CI-APi-LTOF, 1 ml liquid standard HCl (Gaosheng, 36%) and HBr (Macklin, 48%) were diluted in 1000 ml MILLIPORE® ultrapure water resulting in 1.2×10^{-2} mol L^{-1} HCl and 8.6×10^{-3} mol L^{-1} HBr, respectively. Then, 10 ml diluted HCl and HBr solution was put in a U-shape glass tube and then the mixed flow of evaporated HCl and HBr and zero air (1L min^{-1}) went into CI-APi-LTOF (Figure S6). After the injection of gaseous HCl and HBr, the signals of Cl^-, Br^-, $Cl^-\cdot HNO_3$ (or $HCl\cdot NO_3^-$) and $Br^-\cdot HNO_3$ (or $HCl\cdot NO_3^-$) started to increase (Figure S7), confirming that the HCl and HBr can be detected as Cl^-, Br^-, $Cl^-\cdot HNO_3$ (or $HCl\cdot NO_3^-$) and $Br^-\cdot HNO_3$ (or $HBr\cdot NO_3^-$) by CI-APi-LTOF."

Revised text in the main text (line 243-246):

"The background measurement was carried out by sampling zero air. From Figure S7, the background signals were significantly lower than that of ambient air and injected HCl and HBr. The limits of detection (LODs, 3σ) were 1×10^{8} and 1×10^{7} molecules cm^{-3} (i.e., 4 and 0.5 ppt) for HCl and HBr, respectively."

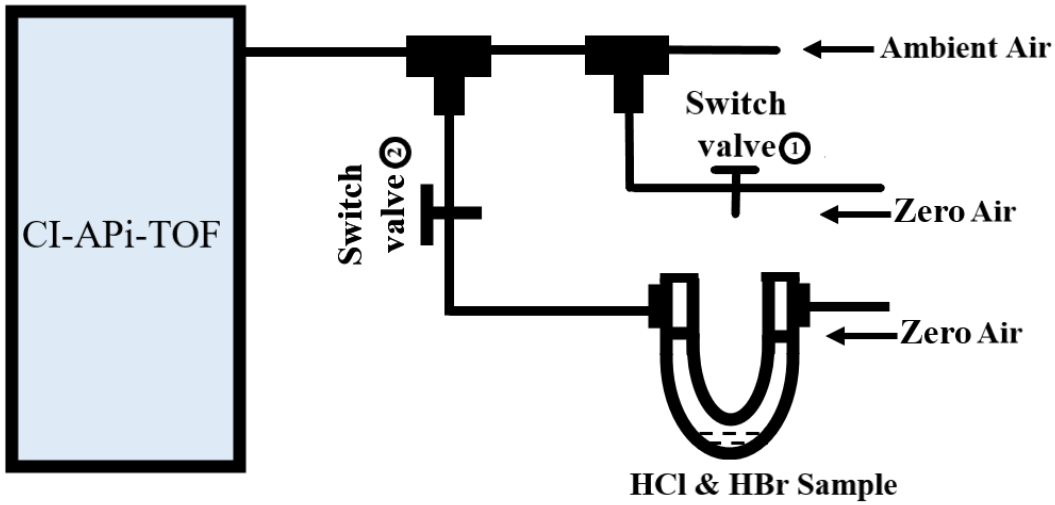

Figure R1 (Figure S6 in revised SI). Schematic of the laboratory experiment set up.

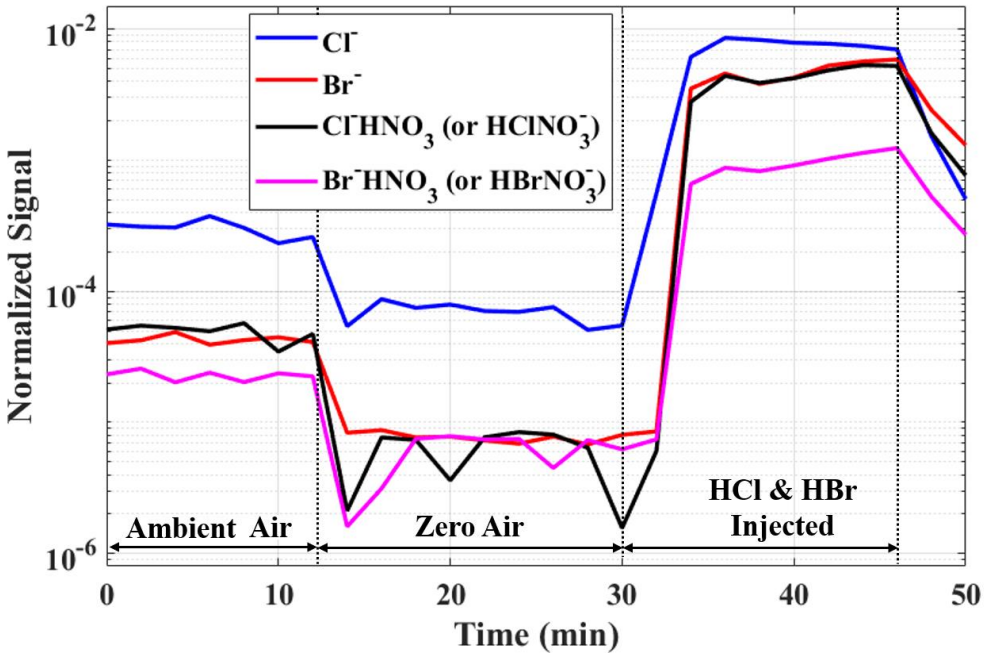

Figure R2 (Figure S7 in revised SI). Time profile of normalized Cl^-, Br^-, $Cl^-{\cdot}HNO_3$ (or $HCl{\cdot}NO_3^-$) and $Br^-{\cdot}HNO_3$ (or $HBr{\cdot}NO_3^-$) signals measured by CI-APi-LTOF during the laboratory test. Within the duration from 0 to 12min, ambient air was sampled and measured by CI-APi-LTOF. The signals of zero air generated from a pure air generator (AADCO 737) were treated as background signals. The detection limits of HCl and HBr were obtained three times the standard deviation of background signals within a 2 min integration time. After the injection of gaseous HCl and HBr which evaporated from HCl and HBr solution, the elevated Cl^-, Br^-, $Cl^-{\cdot}HNO_3$ (or $HCl{\cdot}NO_3^-$) and $Br^-{\cdot}HNO_3$ (or $HBr{\cdot}NO_3^-$) signals were observed.

3. Please clarify the discussion on Lines 287-291 about the correlations between HCl and HBr with temperature and UVB, as the discussion is limited and it is difficult to discern these points

from the figures provided. Also, the authors state that "HCl and HBr concentrations being to increase together with the rising of temperature and UVB during April 2019", but the corresponding Figure 3 only shows data until April 2. Further, in the data shown, the concentration appears to decrease in late March even with higher temperature, showing the opposite of what is discussed in the text.

Reply: To make the sampling period clear, we emphasized our sampling period was from 1 February to 2 April 2019 in the main text and Figure 3 in the revised manuscript.

As pointed out by the reviewer, we did notice that "the concentration appears to decrease in late March even with higher temperature". Yet, the absolute HCl and HBr concentrations are assumed to be affected not only by temperature and UVB, but also by the photochemistry and gas-particle partitioning, indicating by the abundance of HNO_3 (indicated as $[NO_2]$*[OH]) and particulate chloride (Cl (p)), respectively. From revised Figure R3 (Figure 3 in the main text), although the temperature in late March is slightly higher than the beginning of February, the abundant of HNO_3 and particulate chloride in late March is comparatively lower than the beginning of February. The finding of lower Cl(p) concentration in spring than winter is similar to the previous literature in Beijing (Hu et al., 2017) and likely due to fewer combustion emissions. Thus, although in general, the gas/particle ratio increased with temperature (discussed in Major Comments 5 &6), the absolute HCl and HBr concentrations remain at a relatively low level in late March even with higher temperature.

To avoid potential misleading for the readers, we revised the main text as follows (line 305-310):

"For the first period of measurement (from 1 to 15 February), HCl and HBr concentrations are lower when the atmospheric temperature is close to 0℃ and the UVB intensities are relatively low. Yet, for the later period of March, the HCl and HBr concentrations begin to increase along with the rising of temperature and UV. In late March, even with higher temperature, due to the less abundant of HNO_3 and particulate chloride, the HCl and HBr concentrations remain at a relatively low level (Figure 3)."

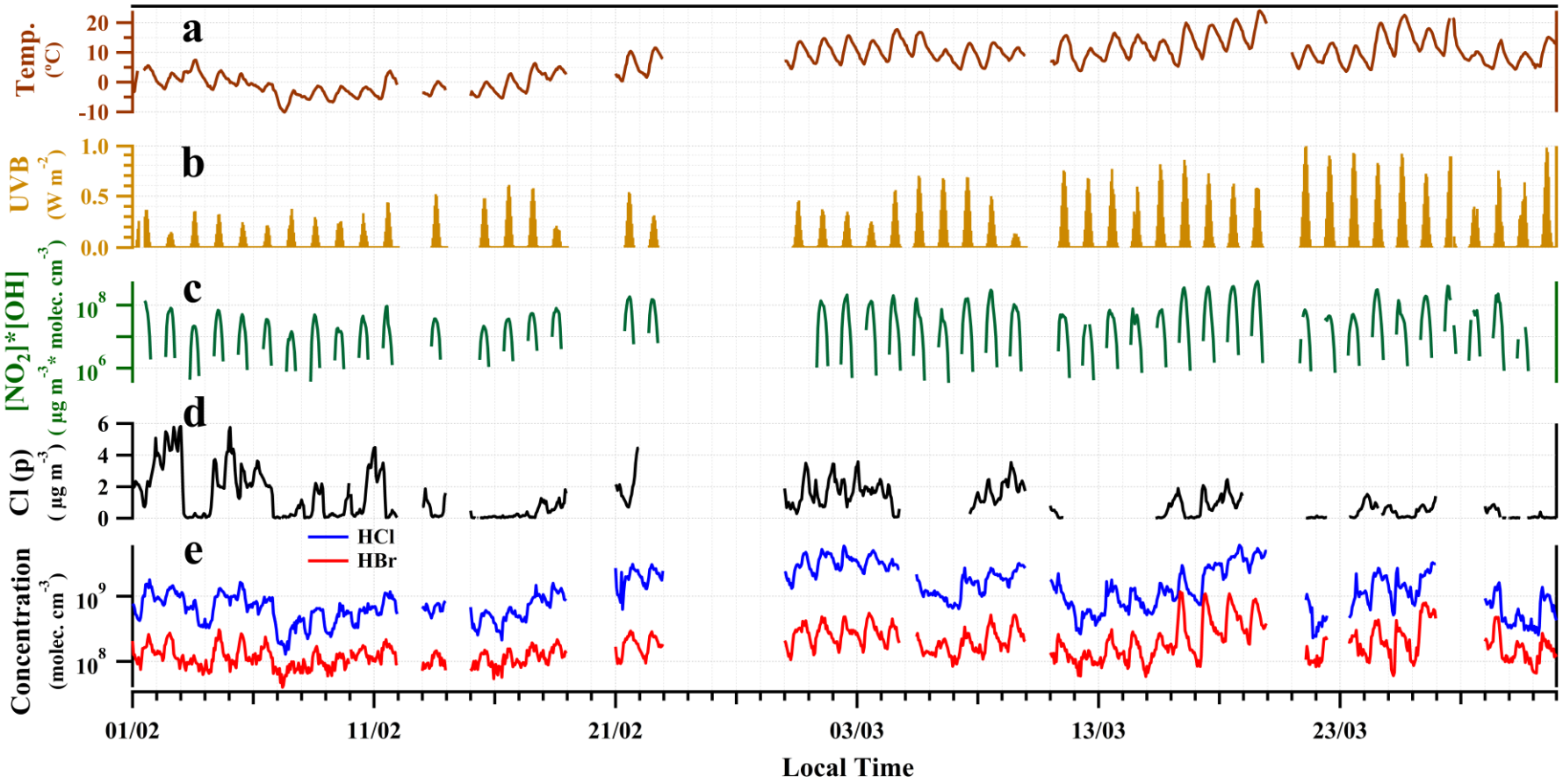

Figure R3 (Figure 3 in revised main text). Time profiles of temperature (**a**), UVB intensities (**b**), $[NO_2]$*[OH] (**c**), particulate chloride (Cl(p)) (**d**), and the mixing ratios of HCl and HBr (**e**). The data points are in hourly-average interval.

4. Throughout the manuscript (including the SI), please clarify whether the particulate chloride discussed is from the ACSM (non-refractory PM1 chloride) or MARGA (total PM2.5 chloride). This differentiation in which particulate chloride is shown may impact the interpretation of the results. It would seem most appropriate to use the MARGA data, but the methods section seems to imply that ACSM data is presented, although this is not clear. Regardless of which data are presented, justification and a quantitative comparison of the ACSM and MARGA chloride data need to be included in the SI. Also, please clarify the text on Lines 276-277, as it suggests as written that the ACSM measured PM2.5 chloride, which is not the case for the standard instrument.

Reply: In this study, we applied an ACSM equipped with a $PM_{2.5}$ aerodynamic lens to present the particulate chloride (Cl(p)) due to the absence of MARGA data during the sampling period. Previous studies have demonstrated that the chloride from ACSM (non-refractory Cl) and online ion chromatography strongly correlated (Canagaratna et al., 2007). From our present study, a high correlation was also observed for particulate Cl between MARGA and ACSM for the later comparison (the same calibration period for CI-API-LTOF and MARGA, r=0.98, intercept=0.067, added in Figure S8). Thus, considering their high correlations, the application of using ACSM to measure particulate Cl during our sampling period is acceptable.

Moreover, the application of $PM_{2.5}$ aerodynamic lens for ACSM, which substantially increased the transmission efficiency for the particles with diameters over 1 μm, has been developed and applied in the heavily polluted areas (Xu et al., 2018; Peck et al., 2016; Zheng et al., 2020). Stable performances were achieved for $PM_{2.5}$ lens ACSM when compared with other online chemical component instruments such as ion chromatography and Sunset OC/EC Analyzer (Zhang et al., 2017).

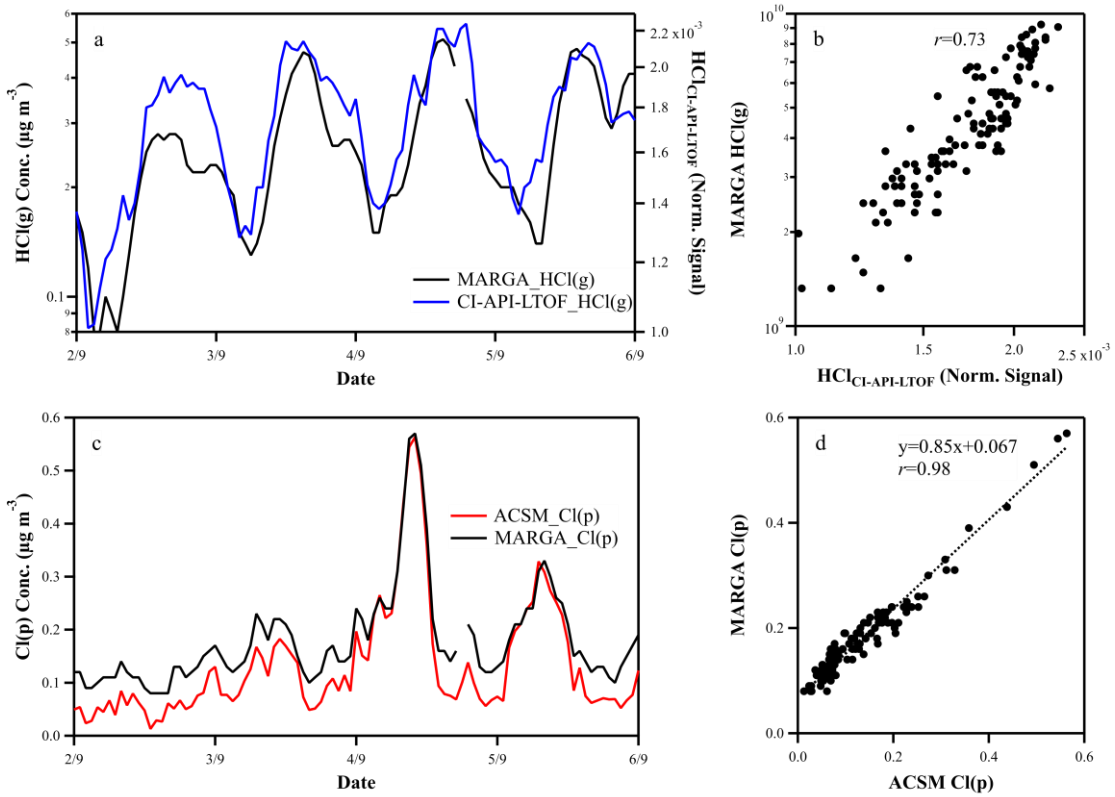

Figure R4 (Figure S8 in revised SI). Time series of normalized HCl signals measured by CI-APi-LTOF and HCl(g) measured by MARGA during the calibration period (i.e., 2 to 6 September 2019) (**a**); The correlation between HCl(g) and normalized HCl signals measured by CI-APi-LTOF (**b**); Time series of particulate Cl (Cl(p)) measured by MARGA and ACSM (**c**); The correlation between particulate Cl (Cl(p)) measured by MARGA and ACSM (**d**).

To clarify the particulate Cl measurement, we revised the description and added the quantitative comparison for ACSM and MARGA to SI (Figure S8, shown above) as suggested in line 244-250. "A time-of-flight aerosol chemical speciation monitor (ToF-ACSM, Aerodyne Research Inc., USA) equipped with a $PM_{2.5}$ aerodynamic lens was applied to measure the particulate non-refractory Cl. The detailed introduction for ToF-ACSM with $PM_{2.5}$ lens and its comparison with other instruments could be found in previous literature (Xu et al., 2017;Zheng et al., 2020;Zhang et al., 2017). Although ACSM only measures the non-refractory Cl, a high correlation was achieved for the comparison between ACSM and MARGA measurement (r=0.98, intercept=0.067, shown in Figure S8d), suggesting non-refractory Cl measured by ACSM could explain a large proportion of particulate Cl in our sampling period."

5. Figure S9 shows the temporal variations in HCl compared to particulate chloride, and this is a key contribution to this work. Therefore, I highly suggest moving this figure to the main text, with the following suggested modifications. Please state in the caption whether ACSM or MARGA Cl- is presented in the figure. In part b, plot both HCl and Cl- as mole ratios for improved comparison

and evaluation of the assertion of gas-particle portioning dominating the diel profile. Then use these mole-based values for a more quantitative discussion on page 7.

Reply: Thanks for the reviewer's suggestion. Figure S9 has been moved to the main text (Figure 5) with the revised figure captions in the revised version. It is now clearly stated the Cl(p) is measured by ACSM. The original panel (c) was also presented as the mole ratio of HCl(g)/Cl(p) as suggested in the new Figure 5b. To better exhibit the quantitative discussions related to gaseous HCl and particulate Cl diurnal variations. We revised the discussion in the main text from line 327 to line 338.

"Our observation of daily averaged mass concentrations of particulate chloride (Cl (p)) in $PM_{2.5}$ showed a similar trend with daily averaged mixing ratios of gaseous HCl (Figure 5a). The difference from the ratios of HCl(g) to Cl(p) in February and March is likely due to the higher temperature in March (Figure 3 and 5a). In contrast, the diurnal variations of HCl and particulate Cl showed the opposite trend at daytime from 08:00 to 17:00 (Figure 5b). The mole ratios of HCl(g) to Cl(p) ranged from <0.1 at nighttime and early morning to >0.3 in the afternoon (Figure 5b). The enhancement of HCl(g)/Cl(p) during the noontime is owing to the large increase of gaseous HCl. It also suggested that the higher temperature and stronger photochemical reactions during the daytime would strongly influence HCl releases from particulate chloride in Beijing, which will be further discussed in the following discussions. During the period between the late afternoon and midnight, the increase of Cl(p) and HCl(g) could be explained by the higher nighttime emissions of residential combustions such as wood and coal burnings in Beijing (Hu et al., 2017;Sun et al., 2016) and high abundance of gaseous HNO_3 are attributed to efficient nocturnal N_2O_5 chemistry (Tham et al., 2018)."

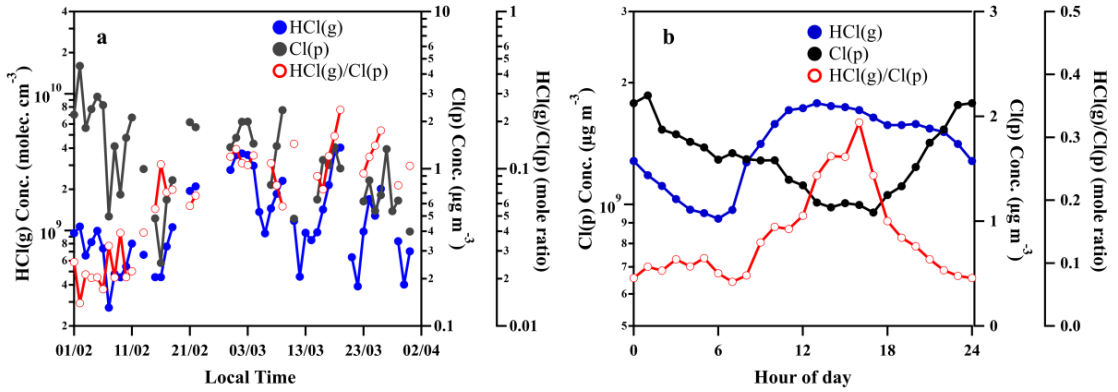

Figure R5 (Figure 5 in revised main text). Time variation of daily averaged concentration of particulate chloride (Cl(p)) measured by ACSM, gaseous HCl (HCl(g)) measured by CI-APi-LTOF and mole ratios of HCl(g)/Cl(p) (**a**) and diurnal variation of HCl(g), Cl (p) and mole ratios of HCl(g)/Cl(p) (**b**).

6. It is stated on Lines 294-295 that HCl and HBr began to increase after sunrise, but the diel plots of Figure 4 do not include radiation for evaluation of this statement. Further, while Figure 3 shows these data as a stacked plot, it is too zoomed out to be able to allow evaluation of this statement. I suggest adding radiation to Figure 4.

Reply: Owing to the total radiations were not recorded during our sampling periods, the UVB intensities were used as alternative ones. The diel plot of UVB (280 - 315 nm) intensities was added to Figure 4 (Figure R6 in this reply) in the main text. From Figure 4 a and b, accompanied by the increasing UVB intensities, the mixing ratios of HCl and HBr started to elevate. The possible driving forces for this would be the increase of atmospheric temperature together with the elevated abundance of HNO_3. From Figure 4d, it is distinct that the partitioning ratios (HCl(g)/Cl(p)) of HCl were enhanced by the high temperature and high abundance of HNO_3, which was indicated as $[NO_2]$*[OH]. Due to the mass concentrations of particulate Br were not measured during our sampling period, a similar plot (Figure 4d) for HBr was not available. Nonetheless, based on the good correlation between HCl and HBr (Figure 4c) and similar diel variations, it is rational to propose that the HBr was also likely affected by the same factors, similar to HCl.

It also should be noted that, during the period between the late afternoon and midnight, the relatively high concentrations of gaseous HCl and HBr still can be observed. One possible reason for this could be that a relatively high abundance of HNO_3 formed from nocturnal NO_3 radical chemistry during this period. Further research is still needed to investigate the effect of NO_3 radical chemistry in the nighttime.

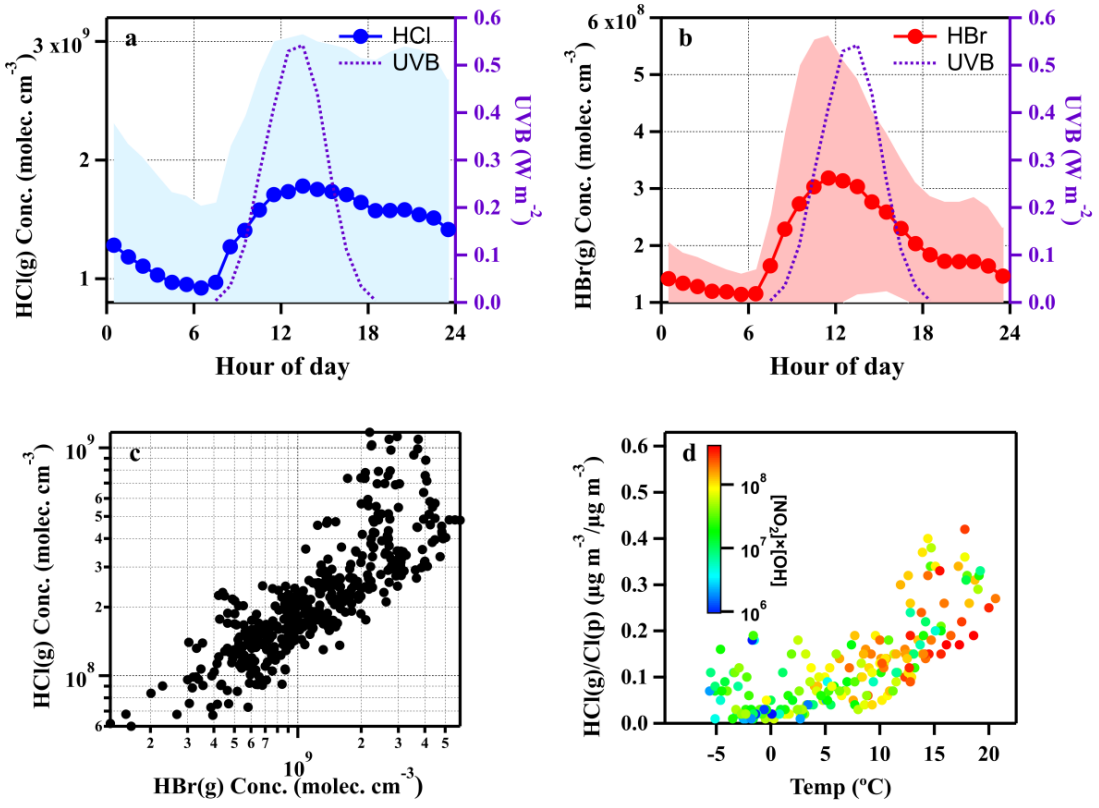

Figure R6 (Figure 4 in the revised main text). Diurnal variations of UVB intensities, HCl and HBr concentrations (averaged values ± one standard deviation) (**a** and **b**) and the correlation between HCl and HBr (**c**). In panel c, the data points are hourly averaged ones during daytime (8:00-17:00). Temperature dependence of gas to particle partitioning ratios of mass concentration of chloride, colour-coded by

[NO_2]*[OH] which was indicated as the abundance of HNO_3 (**d**). All snowy and rainy days during the sampling period were excluded.

7. HBr, similar to HCl, is also formed from the reaction of bromine atoms with hydro-carbons, which would be expected to occur during daylight, when temperature is also higher. It is not clear how the authors are differentiating this process from gas-particle partitioning. Please clarify.

Reply: Yes, the reviewer has a point here. Besides the contribution from gas-particle partitioning, the reaction of bromine atoms with hydrocarbons during the daytime could be another pathway for HBr formation. Unfortunately, without the observation data of other bromine species (e.g., Br_2, $BrNO_2$), it is impossible to differentiate and quantify the contribution by the reaction of bromine atoms with hydrocarbons. Although we cannot exclude the contribution by the reaction of bromine atoms with hydrocarbons to form HBr, this process is likely not the dominant pathway because:

1) Bromine atom is less reactive to hydrocarbons compared to the chlorine atom, and most often reacts with ozone, or reacts with aldehydes (e.g., formaldehyde, which is less abundant, about 20% of the total VOCs, in Beijing) (Simpson et al., 2015; Li et al., 2010).

2) The HBr shows a good correlation with temperature and the HNO_3 precursors ([NO_2]*[OH]), as shown in Figure R3, indicating that the gas-particle partitioning process may be an important process.

Therefore, to make the statement clearer, we decide to revise the statement and add the above information to the revised main text as following:

Line 314-326:

"From Figure 4d, it also can be found that elevated temperature and high abundance of HNO_3 which was indicated as [NO_2]*[OH] could intensify the HCl releases from particulate chloride in the daytime from 08:00 to 17:00. The OH radical concentrations were calculated using J_{NO2} and J_{O1D} (Section S8). This phenomenon is consistent with our observation results above where the increase of temperature and UVB could reinforce the formation of chemicals (e.g., HNO_3) that promote the gas-particle partitioning or directly increase gas-phase formation rate of HCl and HBr (Crisp et al., 2014;Riedel et al., 2012), thus further enhancing the HCl and HBr (Figure 3). Although there is no direct measurement of particulate bromide (Br), considering the similarity in diurnal patterns and good correlation (r = 0.70) between HBr and HCl (Figure 4c), and HBr tracking well with the temperature and [NO_2]*[OH] (see Figure 3), it is rational to suppose HBr also predominantly derived from gas-particle partitioning process. The contribution by the reaction of bromine atoms with hydrocarbons to form HBr is likely not the dominant pathway as bromine atom is less reactive to hydrocarbons compared to the chlorine atom, and most often reacts with ozone (Simpson et al., 2015)."

8. The 24 h air mass trajectory analysis for HBr is not consistent with the typical atmospheric lifetime of 2.5 h reported on Line 129. What is the estimated atmospheric lifetime of HBr under the conditions of this study? Please make sure that the length of the air mass trajectory analysis is appropriate considering the lifetime.

Reply: We noted that the lifetime of HBr was estimated as 2.5h in the previous statement, which is

indeed shorter than the 24h back-trajectory coupled Potential Source Contribution Function (PSCF) analysis. The original purpose of applying back trajectory and PSCF in this study is to point the potential source regions for the air masses that led to high-level concentrations of HBr and HCl during the sampling period. And added the following description and Figure R7 (Figure S9 in revised SI) as a new section (Section S6. PSCF Analysis) in SI line 303-320:

"In PSCF method applied in this study, only the high concentrations of HBr and HCl (>75th percentile, mainly around the middle of the day due to the diurnal patterns) were linked to the trajectories and presented. The 24-h trajectories analysis were conducted by HYSPLIT GDAS data with the ending height of 100 m. PSCF analysis (MeteoInfo PSCF modelling) links the air mass trajectories and high concentrations. The higher potentials of trajectory pathways led to high concentration indicates the possible source regions. Details of PSCF could be found in Wang et al., (2014&2019). The time-series of HBr concentration during the whole sampling period and those applied in the PSCF analysis were exhibited in Figure S9b. It is shown that only the extremely high HBr concentrations were included in the trajectory and PSCF analysis, coincidence with the period of heavy pollution indicated by the high $PM_{2.5}$ concentration level (>80 μg m^{-3} and ~100 μg m^{-3} for HBr and HCl, respectively). Meanwhile, the lower HBr concentrations during the nighttime and clean periods were not included in the PSCF analysis.

Additionally, Cl/Br-containing particles would have a longer lifetime in the atmosphere (from hours to weeks for fine particles in the troposphere (Seinfeld, 2003) and continuously influence the gaseous HBr concentration through gas-particle partitioning. Therefore, in this study, the 24h-backwards air mass trajectory and PSCF analyses were adopted to indicate the source regions of the polluted air masses that result in the high Cl and Br levels rather than the real-time origins of gaseous HCl/HBr in the atmosphere. A shorter time in trajectory analysis, on the other hand, would increase the uncertainties in calculations and may not provide more information on source regions of air parcels at a large scale."

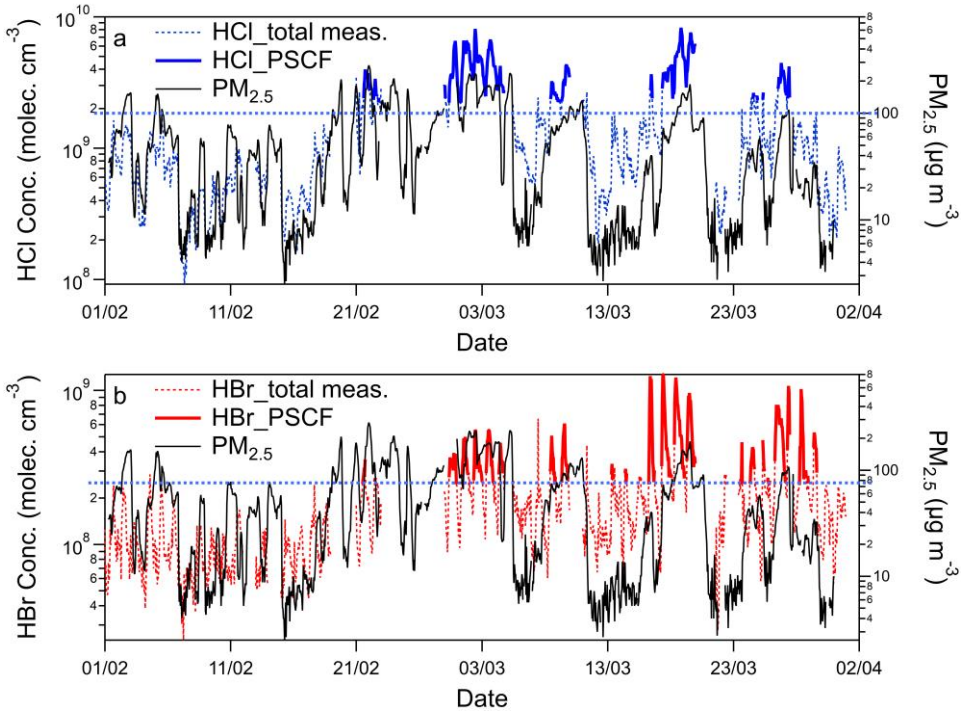

Figure R7 (Figure S9 in revised SI). Time series of gaseous HCl during the whole sampling period, those in PSCF analysis (>75th percentile) and $PM_{2.5}$ mass concentrations (**a**), and gaseous HBr during the whole sampling period, those in PSCF analysis (>75th percentile) and $PM_{2.5}$ mass concentrations (**b**).

To better explain the back trajectory and PSCF analysis, we added the following description in Line 290-296:

"we applied 24h air mass back trajectory and Potential Source Contribution Function (PSCF) analyses to help to elucidate the potential source regions (i.e., air masses) of high levels of HCl and HBr. The detailed descriptions of PSCF and air mass trajectory analysis were described in the SI (Section S6) and previous literature (Wang et al., (2014, 2019b)). It is noted that the lifetime of gaseous HCl and HBr could be shorter than the length of the air mass trajectories. These analyses mainly aimed to point out the source regions of pollutant air masses that brought high levels of Cl and Br rather than the real-time origins of air parcels."

We also revised the figure captions of Figure R8 (Figure 6 in the revised version) accordingly.

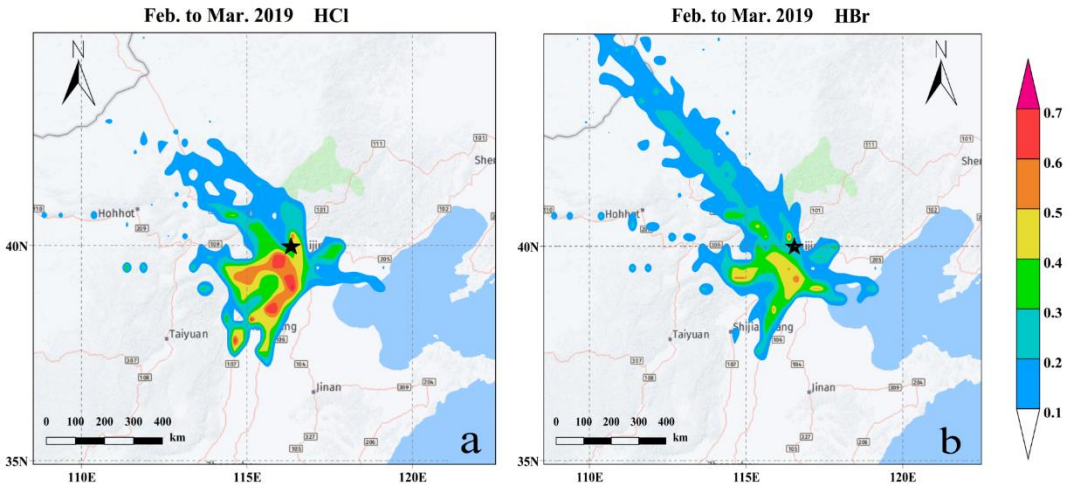

Figure R8 (Figure 6 in revised main text). The results of PSCF analysis for HCl (**a**) and HBr (**b**). Black stars mark the location of the sampling site.

Minor comments

1. Line 56 & elsewhere: Please change "gas-aerosol partitioning" to "gas-particle partitioning".

Reply: "gas-aerosol partitioning" has been changed to "gas-particle partitioning" throughout the manuscript.

2. Introduction, Paragraph 1: The authors are encouraged to also include mercury in the motivation to study atmospheric bromine chemistry.

Reply: Thank you for the suggestion. We have included mercury depletion in the introduction.

Line 98-101:

"Halogen radicals, in particular the atomic chlorine (Cl·) and bromine (Br·), can deplete the O_3, react rapidly with VOCs with reaction rates up to two orders of magnitude faster than that of the hydroxyl radical (OH) reaction with VOCs and accelerate the depletion of gaseous elemental mercury (Atkinson et al., 2007;Calvert and Lindberg, 2004)."

3. Lines 142-144: Additional inland measurements of chlorine chemistry include Mielke et al. 2016 (Can. J. Chem.) and McNamara et al. 2020 (ACS Central Sci.).

Reply: Those two studies have been added to the main text.

Revised text in the main text:

line 141-142: "During the wintertime, the use of road salt could also be a dominant source of atmospheric Cl in the city areas (McNamara et al., 2020)."

line 142-145: "Follow-up studies have confirmed the presence of halogen activation spreading over the continental regions of North America, Canada, Europe and Asia (Mielke et al., 2011;Phillips et al., 2012;Riedel et al., 2013;Tham et al., 2016;Wang et al., 2017;Tham et al., 2018;Liu et al., 2017;Xia et al., 2020;Zhou et al., 2018;McNamara et al., 2020)."

4. Lines 164-165: Please clarify this sentence as it not clear what species are included here, and the manuscript title mentions the stratosphere.

Reply: Thank you for your comment. We noticed that is a typo and has been corrected.

Revised text in the main text (line 165-166):

"The atmospheric bromine is much less abundant than chlorine in the stratosphere with the concentrations of around 25 ppt (parts per trillion by volume) compared to 3.7 ppb of chlorine (Bedjanian and Poulet, 2003)".

5. Lines 178-181 and 312: Note that McNamara et al. 2020 (ACS Central Sci.) also reported inland HCl measurements.

Reply: This study has been involved and introduced in the main text.

Revised text in the main text (line 179-184):

"Some limited studies focused on the atmospheric HCl, for example, Crisp et al. (2014) summarized that the concentration of HCl is typically less than 1 ppb over the continental regions and McNamara et al. (2020) measured the concentration of HCl is around 100 ppt from inland sources, while an airborne measurement showed HCl concentrations of around 100 ppt was typically observed over the land area of northeast United States, except near power plant plumes with concentrations over 1 ppb (Crisp et al., 2014;McNamara et al. 2020;Haskins et al., 2018)."

Revised text in the main text (line 341-344):

"Although it is well known that the HCl is abundant in the polluted coastal and inland regions, previous studies show that the typical HCl mixing ratios over the continental urban areas are less than 1 ppb (Crisp et al., 2014;Faxon and Allen, 2013;Le Breton et al., 2018;McNamara et al. 2020), which are similar to our observations at Beijing."

6. Line 223: Do the authors mean 5 s averaging here, as TOFs operate with much higher time resolution than 5 s.

Reply: TOFs can operate with much higher time resolution, even less than 1 second. Due to our L-TOF was deployed for continuous and long-term ambient measurements, the raw L-TOF data were recorded at 5 s time resolution. For ambient measurements, the 5 s time resolution is sufficient. The data points reported in our manuscript were hourly-averaged ones.

7. Line 302: Please add explanation of Figure 4d to this paragraph to improve the clarity of the discussion here.

Reply: We have added a few sentences to clarify Figure 4d further.

Revised text in the main text (line 314-326):

"From Figure 4d, it also can be found that elevated temperature and high abundance of HNO_3 which was indicated as $[NO_2]$*[OH] could intensify the HCl releases from particulate chloride in the daytime from 08:00 to 17:00. The OH radical concentrations were calculated using J_{NO2} and J_{O1D} (Section S8). This phenomenon is consistent with our observation results above where the increase

of temperature and UVB could reinforce the formation of chemicals (e.g., HNO_3) that promote the gas-particle partitioning or directly increase gas-phase formation rate of HCl and HBr (Crisp et al., 2014;Riedel et al., 2012), thus further enhancing the HCl and HBr (Figure 3). Although there is no direct measurement of particulate bromide (Br), considering the similarity in diurnal patterns and good correlation (r = 0.70) between HBr and HCl (Figure 4c), and HBr tracking well with the temperature and $[NO_2]$*[OH] (see Figure 3), it is rational to suppose HBr also predominantly derived from gas-particle partitioning process. The contribution by the reaction of bromine atoms with hydrocarbons to form HBr is likely not the dominant pathway as bromine atom is less reactive to hydrocarbons compared to the chlorine atom, and most often reacts with ozone (Simpson et al., 2015)."

8. Figure 4: Please consider showing Parts a and b on linear scales in ppt. Part d needs more explanation in the caption. Is this a mass or mole ratio? Also, I did not see measurements of NO2 in the methods section, so are both NO2 and OH calculated values here? Please clarify here in the caption, on Line 374, and SI Line 275 how NO2 was obtained.

Reply: Thanks for the suggestion. Yet, considering the consistency of the unit of manucript and also the suggestions on the units proposed by Reviewer 1#, in Figure 4 in the main text, we still use the unit as "molecules cm^{-3}" but on a linear scale (shown in Figure R6 in Marjor comment 6). We also added the following Figure R9 (Figure S12 in the revised SI) on linear scales in ppt as suggested to help the reader to compare with the studies using the unit of ppt. Figure capations of pandel d is also revised as suggested, which clear stated a mass ratio of HCl(g)/Cl(p) is presented.

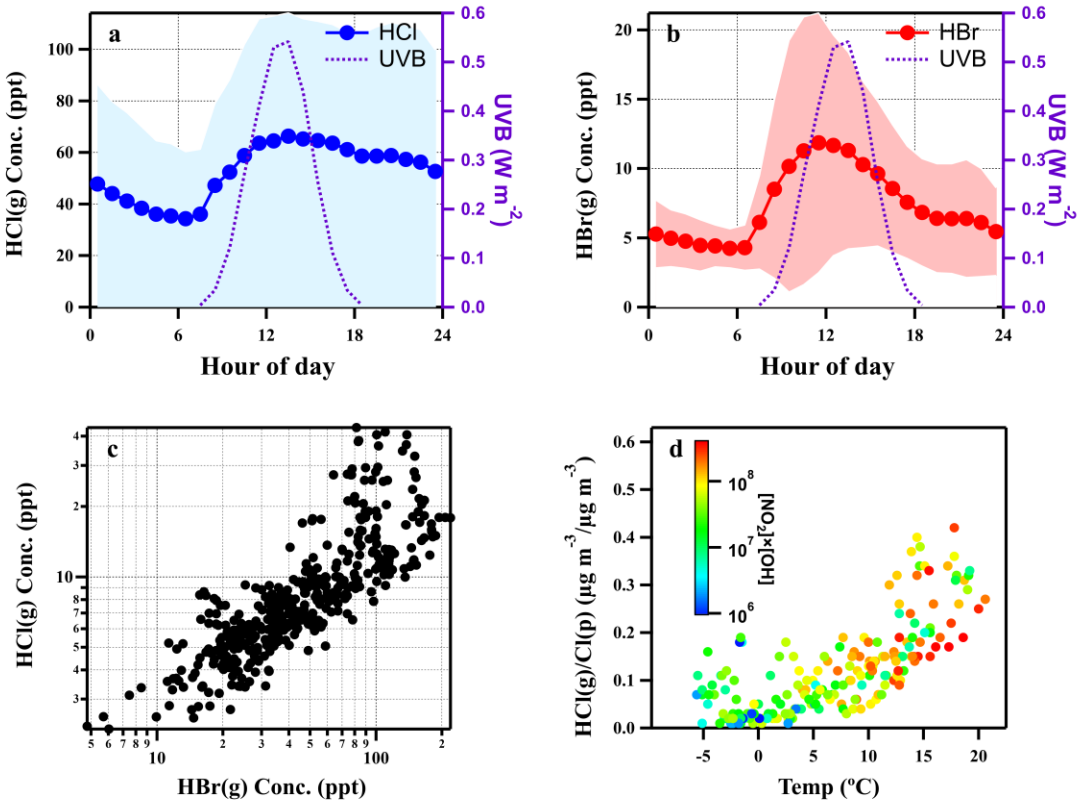

Figure R9 (Figure S12 in the revised SI). Diurnal variations of UVB intensities, HCl and HBr concentrations (averaged values ± one standard deviation) (**a** and **b**) and the correlation between HCl and HBr (**c**). In panel c, the data points are hourly averaged ones during daytime (8:00-17:00). Temperature dependence of gas to particle partitioning ratios of mass concentration of chloride, colour-coded by $[NO_2]$*[OH] which was indicated as the abundance of HNO_3 (**d**). All snowy and rainy days during the sampling period were excluded.

The description of NO_2 measurement "NO_2 was measured with a THERMO 42i NO-NO_2-NO_X Analyzer (Thermal Environment Instruments Inc. USA)" has been added to revised text in line 285-286 and SI (Section S1) line 89-90.

9. Lines 364-366: Please clarify where these measurements were made, as this context is needed for understanding the relevance of the statement.

Reply: Thanks for the comment. We have revised the text and added measurement information as suggested.

Revised text (line 395-400):

"It is also interesting to note that in a previous marine study conducted at Oahu, Hawaii, gaseous Br was found to be 4 to 10 times higher than particulate Br (Moyers and Duce, 1972). On the other hand, from a previous observation conducted in urban Beijing, high levels of both gaseous (7 ng m^{-3}) and particulate (in total suspended particles (TSP), 18 ng m^{-3}) bromine were measured by

offline sampling-organic solvent extraction and Instrumental Neutron Activation Analysis (INAA) method (Tian et al., 2005)."

10. Lines 366-368: Please clarify these sentences. What is meant by extractable gaseous organic bromine? What is the statement "high concentration and reactivity of both organic/inorganic Br" referring to here (as only HBr is presented in this work and organic Br is generally not very reactive)?

Reply: The original expression comes from the reference Tian et al. (2005), which applied Polyurethane Foam Infill (PUF) material to collect the atmospheric gaseous Br and then used organic solvent to extract. The organic solvent-extracted Br were finally analyzed by instrumental neutron activation analysis (INAA) method. Thus, the expression of "extractable gaseous organic bromine" represented the extracted organic Br collected from the offline gas-phase collection. Since the study is not closely related to the HBr measurement in our study, and to avoid possible misleading and confusions, we revised the aforementioned expressions.

Revised text (Line 395-400):

"It is also interesting to note that in a previous marine study conducted at Oahu, Hawaii, gaseous Br was found to be 4 to 10 times higher than particulate Br (Moyers and Duce, 1972). On the other hand, from a previous observation conducted in urban Beijing, high levels of both gaseous (7 ng m^{-3}) and particulate (in total suspended particles (TSP), 18 ng m^{-3}) bromine were measured by offline sampling-organic solvent extraction and Instrumental Neutron Activation Analysis (INAA) method (Tian et al., 2005)."

11. Lines 375-378: Note that McNamara et al 2020 (ACS Central Sci) also reported similar Cl atom production rates from OH + HCl for the inland urban environment.

Reply: This study has been included in the discussion.

Revised text in the main text (line 409-410):

"These rates fall within the range of Cl atom production rates (~10^3 to 10^6 molecules cm^{-3} s^{-1}) reported in polluted environments (Crisp et al., 2014;Hoffmann et al., 2018;McNamara et al 2020)."

12. Lines 382-383: Please provide references for this statement of previous work and also compare the Cl atom production rates from HCl in this work to ClNO2 and Cl2 photolysis in the previous studies.

Reply: Agree. The text has been revised as the following (line 420- 425):

"Recent studies in several polluted sites of China suggested that the photolysis of $ClNO_2$ and Cl_2 are the dominant daytime Cl atom sources leading to Cl atom production rate up to 8×10^6 molecules cm^{-3} s^{-1} (Tham et al., 2016;Liu et al., 2017;Xia et al., 2020), while our observation of Cl atom production rate from HCl + OH is about 2×10^3 molecules cm^{-3} s^{-1}. Despite the lower production rate, the reaction of HCl with OH may also act as important recycling of Cl atom, which ultimately enhanced the atmospheric oxidation capacity (Riedel et al.,2012)."

13. Line 387: This statement about the ubiquity of bromine chemistry in the polluted urban

environment is speculative and not supported by the paper cited.

Reply: We agree with the reviewer that the ubiquity of bromine chemistry in the polluted urban environment is speculative because there is no previous study that reported such species in the urban environment. However, a recent study found that Br_2 and BrCl are ubiquitous in the polluted environment of China which is influenced by biomass burning (Peng et al., 2020). This result together with the results from Lee et al. (2018) paper point to the fact that both biomass burning and coal-fired power plant are the major sources of bromine and these sources are quite widespread in the polluted environment of China. Therefore, we believe that bromine chemistry is ubiquitous in a polluted urban environment. We have tone down the statement and the revised sentence is as the following.

Line 425-429:

"In analogous to the chlorine chemistry, the reaction of HBr with OH could be a significant source of Br atom in the daytime although rapid photolysis of Br_2 and $BrNO_2$ is believed to be the major Br atom source in a polluted urban environment as ubiquitous bromine species (e.g. Br_2, BrCl and $BrNO_2$) have been previously observed in residential coal burning and coal-fired power plant plumes (Lee et al., 2018;Peng et al., 2021)."

14. Lines 499-503: This reference is listed twice.

Reply: The reference list has been corrected.

15. Figure 1: The font on these maps is not readable as currently presented.

Reply: Thanks for the suggestions and Figure 1 has already been changed accordingly.

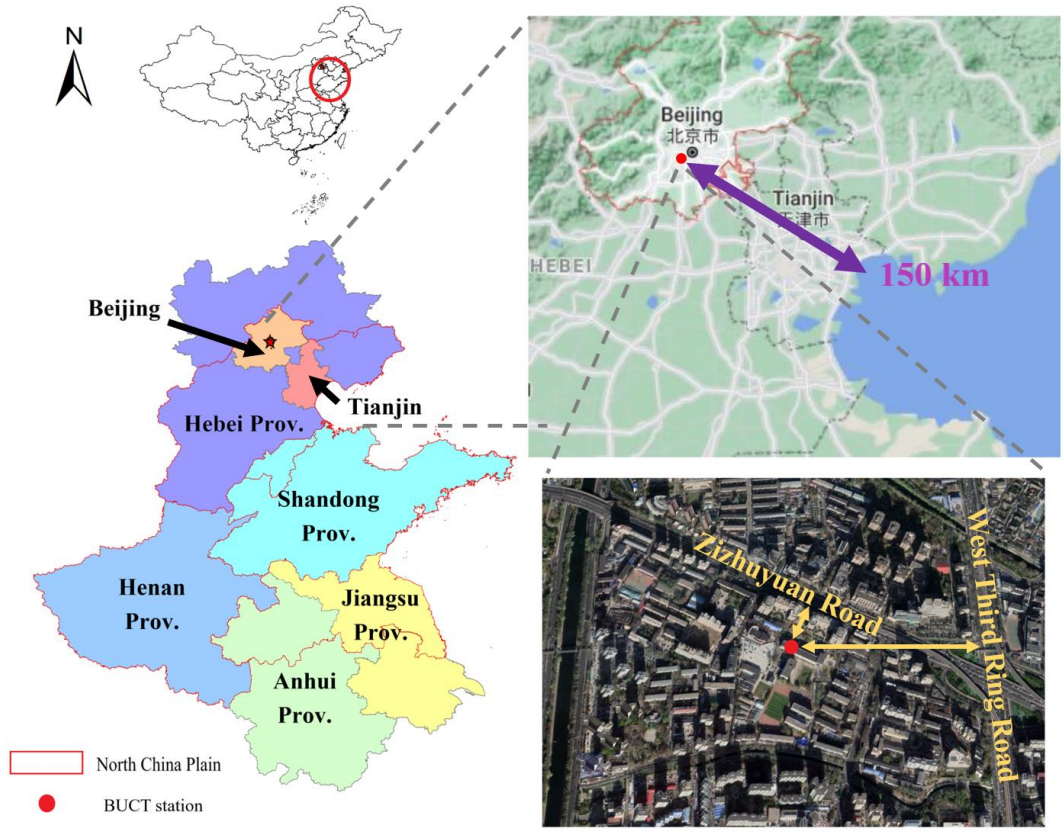

Figure R10 (Figure 1 in revised main text). The location of BUCT measurement station. The satellite map was revised from © Google map.

16. Figure 2: Consider showing HCl on the left axis and HBr on the right axis, both on linear scales. Incorporate measurement uncertainty.

Reply: Figure 2 has already been changed accordingly and the updated Figure 2 was also attached here.

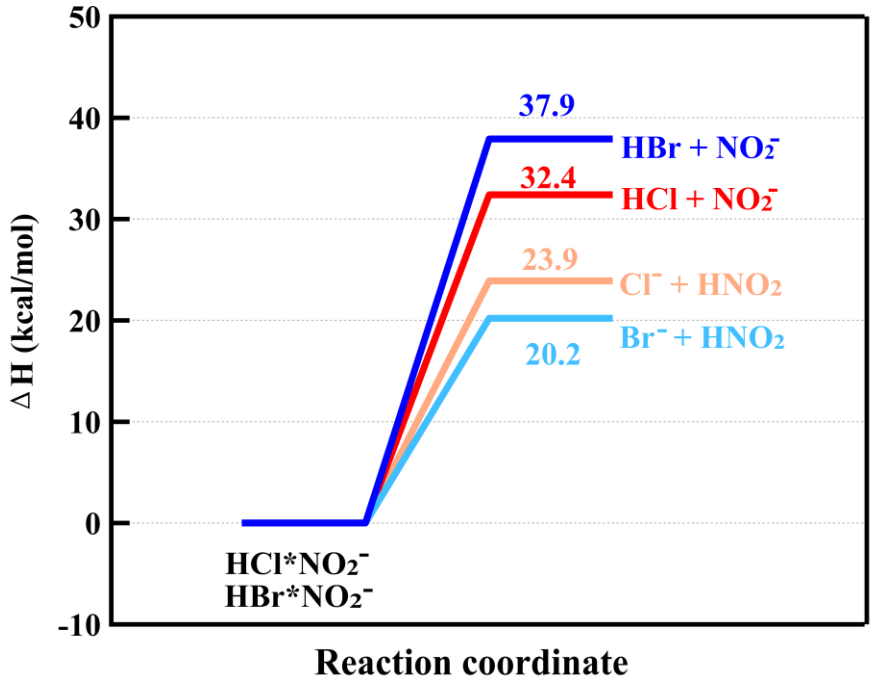

Figure R11 (Figure 2 in revised main text). The calculated enthalpy of $HCl{\cdot}NO_2^-$ formed by HCl with NO_2^- and Cl^- with HNO_2 and enthalpy of $HBr{\cdot}NO_2^-$ formed by HBr with NO_2^- and Br^- with HNO_2 at the DLPNO-CCSD(T)/def2-QZVPP// ωB97X-D/aug-cc-pVTZ-PP level of theory.

17. Figure 7: Please clarify in the caption that all of the 'data' shown are calculations, not measurements, as implied by the text in the caption.

Reply: The figure and its caption were revised accordingly. The revised caption:

"Time series of calculated production rates of Cl and Br radicals during the observation period (**a**); diurnal variations of HCl and HBr concentrations in clean and polluted days (**b**); diurnal variations of production rates of Cl and Br radicals, together with calculated OH radical concentrations (**c**) and production rates of Cl and Br radicals in clean and polluted days (**d**). The clean and polluted days were classified as daily $PM_{2.5} < 75$ μg/m^3 and $PM_{2.5} \geq 75$ μg/m^3, respectively. The data points are in the hourly-average interval and measured during observation periods from 1 February to 31 March 2019."

References:

Calvert, J and Lindberg, S.: The potential influence of iodine-containing compounds on the chemistry of the troposphere in the polar spring. II. Mercury depletion. Atmospheric Environment 38(30), 5105-5116, 2004.

Canagaratna, M. R., Jayne, J. T., Jimenez, J. L., Allan, J. D., Alfarra, M. R., Zhang, Q., Onasch, T. B., Drewnick, F., Coe, H., Middlebrook, A., Delia, A., Williams, L. R., Trimborn, A. M., Northway, M. J., DeCarlo, P. F., Kolb, C. E., Davidovits, P., and Worsnop, D. R.: Chemical and microphysical characterization of ambient aerosols with the aerodyne aerosol mass spectrometer, Mass Spectrom Rev, 26, 185-222, 10.1002/mas.20115, 2007.

Du, H.H., Kong, L.D., Cheng,T.T., Chen, J.M., Yang, X., Zhang, R.Y., Han,Z.W., Yan, Z., Ma, Y.L.: Insights into ammonium particle-to-gas conversion: non-sulfate ammonium coupling with nitrate and chloride. Aerosol Air Qual. Res. 10, 589–595, 2010

Du, H.H., Kong, L.D., Cheng, T.T., Chen, J.M., Du, J.F., Li, L., Xia, X.G., Leng, C.P., Huang, G.H.: Insights into summertime haze pollution events over Shanghai based on online water-soluble ionic composition of aerosols. Atmos. Environ. 45, 5131–5137, 2011

Hu, W., Hu, M., Hu, W. W., Zheng, J., Chen, C., Wu, Y. S., and Guo, S.: Seasonal variations in high time-resolved chemical compositions, sources, and evolution of atmospheric submicron aerosols in the megacity Beijing, Atmospheric Chemistry and Physics, 17, 9979-10000, 10.5194/acp-17-9979-2017, 2017.

Li, Y. , Shao, R. , Lu, R. , Chang, R. C. , & Dasgupta, R. K.: Variations and sources of ambient formaldehyde for the 2008 Beijing Olympic games. Atmospheric Environment, 44(21-22), 2632-2639, 2010.

Peck, J., Gonzalez, L. A., Williams, L. R., Xu, W., Croteau, P. L., Timko, M. T., Jayne, J. T., Worsnop, D. R., Miake-Lye, R. C., and Smith, K. A.: Development of an aerosol mass spectrometer lens system for PM2.5, Aerosol Science and Technology, 50, 781-789, 10.1080/02786826.2016.1190444, 2016.

Peng, X., Wang, W., Xia, M., Chen, H., Ravishankara, A. R., Li, Q., Saiz-Lopez, A., Liu, P., Zhang, F., Zhang, C., Xue, L., Wang, X., George, C., Wang, J., Mu, Y., Chen, J., and Wang, T.: An unexpected large continental source of reactive bromine and chlorine with significant impact on wintertime air quality, National Science Review, 10.1093/nsr/nwaa304, 2020

Seinfeld, J. H.: TROPOSPHERIC CHEMISTRY AND COMPOSITION | Aerosols/Particles, in: Encyclopedia of Atmospheric Sciences, edited by: Holton, J. R., Academic Press, Oxford, 2349-2354, 2003.

Sun, Y., Du, W., Fu, P., Wang, Q., Li, J., Ge, X., Zhang, Q., Zhu, C., Ren, L., Xu, W., Zhao, J., Han, T., Worsnop, D. R., and Wang, Z.: Primary and secondary aerosols in Beijing in winter: sources, variations and processes, Atmospheric Chemistry and Physics, 16, 8309-8329, 10.5194/acp-16-8309-2016, 2016.

Tian, Q., Xu, D., Chai, Z., Lu, Y., and Xiong, Y.: Analysis on the organic bromine in the atmosphere in Beijing, Journal of Nuclear and Radiochemistry, 27, 236-238,252, 2005.

Trebs, I., Meixner, F., Slanina, J., Otjes, R., Jongejan, P., and Andreae, M.: Real-time measurements of ammonia, acidic trace gases and water-soluble inorganic aerosol species at a rural site in the Amazon Basin, Atmospheric Chemistry and Physics, 4, 967-987, 10.5194/acp-4-967-2004, 2004.

Wang, L., Du, H., Chen, J.-M., Zhang, M., Huang, X., Tan, H., Kong, L., and Geng, F.: Consecutive transport of anthropogenic air masses and dust storm plume: Two case events at Shanghai, China, Atmospheric Research, 127, 22–33, 10.1016/j.atmosres.2013.02.011, 2013.

Wang, Y. Q.: MeteoInfo: GIS software for meteorological data visualization and analysis, Meteorological Applications, 21, 2014.

Wang, Y. Q.: An Open Source Software Suite for Multi-Dimensional Meteorological Data Computation and Visualisation, Journal of Open Research Software, 7, 10.5334/jors.267,

2019.
Xu, W., Croteau, P., Williams, L., Canagaratna, M., Onasch, T., Cross, E., Zhang, X., Robinson, W., Worsnop, D., and Jayne, J.: Laboratory characterization of an aerosol chemical speciation monitor with PM2.5 measurement capability, Aerosol Science and Technology, 51, 69-83, 10.1080/02786826.2016.1241859, 2017.
Xu, W., Lambe, A., Silva, P., Hu, W. W., Onasch, T., Williams, L., Croteau, P., Zhang, X., Renbaum-Wolff, L., Fortner, E., Jimenez, J. L., Jayne, J., Worsnop, D., and Canagaratna, M.: Laboratory evaluation of species-dependent relative ionization efficiencies in the Aerodyne Aerosol Mass Spectrometer, Aerosol Science and Technology, 52, 626-641, 10.1080/02786826.2018.1439570, 2018.
Zhang, Y., Tang, L., Croteau, P. L., Favez, O., Sun, Y., Canagaratna, M. R., Wang, Z., Couvidat, F., Albinet, A., Zhang, H., Sciare, J., Prévôt, A. S. H., Jayne, J. T., and Worsnop, D. R.: Field characterization of the $PM_{2.5}$ Aerosol Chemical Speciation Monitor: insights into the composition, sources, and processes of fine particles in eastern China, Atmospheric Chemistry and Physics, 17, 14501-14517, 10.5194/acp-17-14501-2017, 2017.
Zheng, Y., Cheng, X., Liao, K., Li, Y., Li, Y. J., Huang, R.-J., Hu, W., Liu, Y., Zhu, T., Chen, S., Zeng, L., Worsnop, D. R., and Chen, Q.: Characterization of anthropogenic organic aerosols by TOF-ACSM with the new capture vaporizer, Atmospheric Measurement Techniques, 13, 2457-2472, 10.5194/amt-13-2457-2020, 2020.

Atmospheric gaseous hydrochloric and hydrobromic acid in urban Beijing, China: detection, source identification and potential atmospheric impacts

Xiaolong Fan[1#], Jing Cai[2#], Chao Yan[2], Jian Zhao[2], Yishuo Guo[1], Chang Li[1], Kaspar R. Dällenbach[2], Feixue Zheng[1], Zhuohui Lin[1], Biwu Chu[3,4], Yonghong Wang[2], Lubna Dada[2], Qiaozhi Zha[2], Wei Du[2], Jenni Kontkanen[2], Theo Kurtén[5], Siddhart Iyer[6], Joni T Kujansuu[1,2], Tuukka Petäjä[2], Douglas R. Worsnop[7], Veli-Matti Kerminen[2], Yongchun Liu[1], Federico Bianchi[2], Yee Jun Tham[8,2*], Lei Yao[2*], Markku Kulmala[1,2,9]

Affiliations:

[1]Aerosol and Haze Laboratory, Beijing Advanced Innovation Center for Soft Matter Science and Engineering, Beijing University of Chemical Technology, Beijing 100089, China

[2] Institute for Atmospheric and Earth System Research / Physics, Faculty of Science, University of Helsinki 00560, Finland

[3] State Key Joint Laboratory of Environment Simulation and Pollution Control, Research Center for Eco-Environmental Sciences, Chinese Academy of Sciences, Beijing 100085, China

[4] Center for Excellence in Regional Atmospheric Environment, Institute of Urban Environment, Chinese Academy of Sciences, Xiamen 361021, China

[5] Department of Chemistry, University of Helsinki, FI-00014 Helsinki, Finland

[6] Aerosol Physics Laboratory, Physics Unit, Tampere University, Tampere 33100, Finland

[7] Aerodyne Research Inc., Billerica, Massachusetts 01821, USA

[8] School of Marine Sciences, Sun Yat-Sen University, Zhuhai 519082, China

[9] Joint International Research Laboratory of Atmospheric and Earth System Sciences (JirLATEST), Nanjing University, Nanjing 210023, China.

[#] These authors contributed equally.

Correspondence: Lei Yao (lei.yao@helsinki.fi) and Yee Jun Tham (thamyj@mail.sysu.edu.cn)

Abstract

Gaseous hydrochloric (HCl) and hydrobromic acid (HBr) are vital halogen species that play essential roles in tropospheric physicochemical processes. Yet, the majority of the current studies on these halogen species were conducted in marine or coastal areas. Detection and source identification of HCl and HBr in inland urban areas remain scarce, thus, limiting the full understanding of halogen chemistry and potential atmospheric impacts in the environments with limited influence from the marine sources. Here, both gaseous HCl and HBr were concurrently measured in urban Beijing, China during winter and early spring of 2019. We observed significant HCl and HBr concentrations ranged from a minimum value at 1×10^{8} molecules cm^{-3} (4 ppt) and 4×10^{7} molecules cm^{-3} (1 ppt) up to 6×10^{9} molecules cm^{-3} (222 ppt) and 1×10^{9} molecules cm^{-3} (37 ppt)1.3×10⁸ molecules cm⁻³ (54 ppt) and 4.34.3×10⁷ molecules cm⁻³ (21 ppt) up to 5.95.96×10⁹ molecules cm⁻³ (219.22 ppt) and 1.2.2×10⁹ molecules cm⁻³ (3744 ppt), respectively. The HCl and HBr concentrations are enhanced along with the increase of atmospheric temperature, UVB, and levels of gaseous HNO_3. Based on the air mass analysis and high correlations of HCl and HBr with the burning indicators (HCN and HCNO), the gaseous HCl and HBr are found to be related to anthropogenic burning aerosols. The gas-aerosol particle partitioning may also play a dominant role in the elevated daytime HCl and HBr. During the daytime, the reaction of HCl and HBr with OH radicals lead to significant production of atomic Cl and Br, up to 2×10^{4} molecules cm^{-3} s^{-1} and 8×10^{4} molecules cm^{-3} s^{-1}2×10⁴ molecules cm⁻³ s⁻¹and 7.98×10⁴ molecules cm⁻³ s⁻¹, respectively. The production rate of atomic Br (via HBr + OH) are 2-3 times higher than that of atomic Cl (via HCl + OH), highlighting the potential importance of bromine chemistry in the urban area. In polluted days, the production rates of atomic Cl and Br are faster than those on clean days. In polluted days, the production rates of atomic Cl and Br are faster than that on clean days. Furthermore, our observations of elevated HCl and HBr may suggest an important recycling pathway of halogen species in inland megacities, and may provide a plausible explanation for the widespread of halogen chemistry, which could affect the atmospheric oxidation in China.

1. Introduction

Tropospheric halogen chemistry plays variety of roles in perturbing the fate of chemical compositions, including ozone (O_3) and volatile organic compounds (VOCs) in the troposphere (Saiz-Lopez and von Glasow, 2012;Simpson et al., 2015;-Artiglia et al., 2017). Halogen radicals, in particular the atomic chlorine (Cl·) and bromine (Br·), can deplete the O_3, –react rapidly with VOCs with reaction rates up to two orders of magnitude faster than that of the hydroxyl radical (OH) reaction with VOCs ~~(Atkinson et al., 2007)~~ and accelerate~~e~~ the depletion of gaseous elemental mercury ~~.~~(Atkinson et al., 2007; Calvert and Lindberg, 2004-). Significant halogen-induced O_3 reduction of about 10% of the annually averaged tropospheric ozone column was reported over the tropical marine boundary layer (Saiz-Lopez et al., 2012). However, in polluted coastal regions with high NO_x, the coupling between halogen chemistry and NO_x chemistry contributes to significant enhancement of ozone production of up to 7 ppb (parts per billion by volume) (Li et al., 2020;Sherwen et al., 2017;Sarwar et al., 2014). Besides affecting the ozone chemistry, the oxidation processes of VOCs by halogen radicals can potentially lead to secondary aerosols production. Wang and Hildebrandt Ruiz ~~(2017)~~ demonstrated that the chlorine-initiated oxidation of isoprene contributed to the formation of particulate organochloride and the yield of secondary organic aerosol (SOA) ranged from 7 to 36% (Wang and Ruiz, 2017). A recent study also found that the oxidation of alpha-pinene by chlorine atoms yields low-volatility organic compounds, which are essential precursors for secondary particle formation and growth (Wang et al., 2020).

It is known that sea-salt particle is a major source of atomic halogens in the marine environment. The chloride (Cl^-) and bromide (Br^-) in the sea-salt particles can be displaced by strong acids (i.e., nitric acid (, HNO_3) and sulfuric acid (H_2SO_4)) to release gas-phase hydrogen halides HX (reaction (R1); X = Cl or Br) into the atmosphere (Gard et al., 1998;Thornton et al., 2010). The HX then can react with an OH radical to form a X· via reaction (R2).

$$X^-\text{ (sea-salt)} + HNO_3 \rightarrow HX \quad \text{(R1)}$$

$$HX + OH \rightarrow X\cdot + H_2O \quad \text{(R2)}$$

On the other hand, the heterogeneous uptake of dinitrogen pentoxide (N_2O_5) onto sea-salt particles can form nitryl halides XNO_2 via reaction (R3) (Finlayson-Pitts et al., 1989;Osthoff et al., 2008;Tham et al., 2014), which is a reservoir of halogen during the nighttime. At sunrise, the XNO_2 undergoes rapid photolysis to liberate highly reactive halogen atom (X·), which subsequently reacts with VOCs to produce HX and peroxy radicals (RO_2; reaction (R4) and (R5)). Besides, the heterogeneous oxidation of Br^- by O_3 at the aqueous phase-vapour interface can lead to the formation of a pre-complex intermediate ($Br\cdot OOO^-$) which contributes the formation of atmospheric HOBr (Artiglia et al., 2017).

$$X^-\text{ (sea-salt)} + N_2O_5 \rightarrow XNO_2 + NO_3^- \quad \text{(R3)}$$

$$XNO_2 + h\nu \rightarrow X\cdot + NO_2 \quad \text{(R4)}$$

$$X\cdot + RH \rightarrow HX + RO_2 \quad \text{(R5)}$$

The atmospheric lifetimes of HCl and HBr due to reaction (R2) are approximately 35.6 h and 2.5 h (when OH = 1×10^7 ~~molecule~~molecules ~~-~~cm^{-3}), respectively, making them a significant daytime recycling source of atomic halogen in the marine atmosphere. Riedel et al. (2012) showed that the reaction of HCl with OH accounts for about 45% of the integrated Cl atom production over the entire day along the Santa Monica Bay of Los Angeles (Riedel et al., 2012). Another ship-borne study reported that the Cl atom production rate peaks at ~~3~~3×10^5 ~~molecule~~molecules ~~s~~ cm^{-3} s^{-1} during the noontime in Southern Coastal California (Crisp et al., 2014). The produced HCl and HBr can also end up in particle phase during the nighttime (Chen et al., 2016;Roberts et al., 2019;Crisp et al., 2014), and further promoting the heterogeneous reaction of N_2O_5 (R3).

The discovery of Thornton et al. (2010) has changed the paradigm of halogen chemistry, where it was thought to be restricted to the marine environment (Thornton et al., 2010). A significant source of atomic chlorine from the heterogeneous reaction of N_2O_5 onto chloride aerosol (R3) was observed in Boulder, U.S., which is 1400 km from the nearest coastline, indicating that active chlorine chemistry also occurs in the region far from the ocean (Thornton et al., 2010). During the wintertime, the use of road salt could also be a dominant source of atmospheric Cl in the city areas (McNamara et al., 2020). Follow-up studies have confirmed the presence of halogen activation spreading over the continental regions of North America, Canada, Europe and Asia (Mielke et al., 2011;Phillips et al., 2012;Riedel et al., 2013;Tham et al., 2016;Wang et al., 2017;Tham et al., 2018;Liu et al., 2017;Xia et al., 2020;Zhou et al., 2018; McNamara et al., 2020). These findings suggest a crucial role for HCl gas-particle partitioning in sustaining the aerosol chloride concentrations in continental regions for reaction (R3) to take place (Brown and Stutz, 2012).

On the global scale, sea salt sprays were estimated to be the dominant source of halogens such as Cl and Br (Wang et al., 2019a;Keene et al., 1999). Through acid displacement and other heterogeneous processes, 64 Tg a^{-1} and 6.2 Tg a^{-1} gas-phase inorganic Cl and Br from sea salt were emitted to the troposphere, while anthropogenic emissions such as biomass burning, fossil combustion and incineration were supposed to be minor on a global scale (Wang et al., 2019a;Keene et al., 1999). For the emissions of Cl, anthropogenic emissions were quite crucial for both gaseous and particulate Cl in the urban environment and heavily polluted areas. For example, the anthropogenic emissions for gaseous HCl and particulate Cl were 458 and 486 Gg in 2014 in China, of which biomass burning is the largest contributor (Fu et al., 2018~~a~~). Many recent field studies reported elevated $ClNO_2$ and particulate chloride concentrations in the plumes influenced by biomass burning and coal-fired power plants, suggesting they could be the driving force for the Cl activation process in continental areas (Riedel et al., 2013;Tham et al., 2016;Wang et al., 2017;Liu et al., 2017;Yang et al., 2018). Furthermore, Bannan et al.(2019) showed that the $ClNO_2$ is consistently formed at a landfill site in London, highlighting the potential contribution from landfill emissions of Cl in promoting the reactions (R3) and (R4) (Bannan et al., 2019). Other possible anthropogenic Cl sources include the emissions from industrial, and water and sewage treatment plants (Hara et al., 1989;Graedel and Keene, 1995;Thornton et al., 2010). During the wintertime, the use of road salt could also be a dominant source of atmospheric Cl in the city areas (McNamara et al., 2020).

The atmospheric bromine is much less abundant than chlorine in the stratosphere ~~troposphere~~ with the concentrations of around 25 ppt (parts per trillion by volume) compared to 3.7 ppb of chlorine (Bedjanian and Poulet, 2003). HBr is known as a principal bromine sink species for the ozone loss chemistry in the stratosphere showing the average concentration of 1.3±0.39 ppt between 20.0 to 36.5 km altitude (Bedjanian and Poulet, 2003;Nolt et al., 1997;Yang et al., 2005), and also one of the dominant inorganic bromine species in the marine boundary layer, free troposphere and tropical tropopause layer as well (Fernandez et al., 2014;Glasow and Crutzen, 2014;Nolt et al., 1997;Bedjanian and Poulet, 2003). In the urban environment, atmospheric Br was previously known to be strongly affected by traffic emissions since ethylene dibromide ($C_2H_4Br_2$) was used to be as anti-knock compounds to leaded gasoline (Glasow and Crutzen, 2014). Yet, since the phasing out of leaded gasoline, the long-term atmospheric Br exhibited a continuous decreasing trend for 2 to 3 decades ~~atmospheric Br~~ in Germany (Lammel et al., 2002), and a similar situation is expected in Beijing as the usage of leaded gasoline was banned from the years around the 2000s in China (Cai et al., 2017).

Despite the advances in the understanding of concentrations and sources of global halogen species, the atmospheric gaseous HCl and HBr in the continental, especially urban environments, are much less studied. Some limited studies focused on the atmospheric HCl, for example, Crisp et al. (2014) summarized that the

concentration of HCl is typically less than 1 ppb over the continental regions and McNamara et al. (2020) measured the concentration of HCl is around 100 ppt from inland sources~~Crisp et al.(2014) (Crisp et al., 2014) summarized that the concentration of HCl is typically less than 1 ppb over the continental regions (Crisp et al., 2014) and McNamara et al. (2020) measured the concentration of HCl is around 100 ppt from inland sources (McNamara et al. 2020)~~, while an airborne measurement showed HCl concentrations of around 100 ppt was typically observed over the land area of northeast United States, except near power plant plumes with concentrations over 1 ppb (Crisp et al., 2014;McNamara et al. 2020;Haskins et al., 2018). Furthermore, much less information is available on the presence of HBr in the continental environment. Until very recently, an airborne measurement detected significant levels of gas-phase reactive bromine species in the exhaust of coal-fired power plants (Lee et al., 2018). Therefore, the measurement of gas-phase HCl and HBr in inland urban environments is of necessary to fully assess their effects on the tropospheric chemistry, such as gas-particle partitioning effects on the particulate halide concentrations that can undergo rapid activation via reaction (R3). Those would be more important in polluted regions such as the North China Plain, where Beijing is located in and a large amount of chloride were emitted to the atmosphere (Tham et al., 2016;Zhou et al., 2018;Fu et al., 2018~~b~~).

In this study, we deployed a Chemical Ionization-Atmospheric Pressure interface-long-Time-Of-Flight mass spectrometer (CI-APi-LTOF) to measure the atmospheric gas-phase HCl and HBr from 1 February~~1~~ to 31 March~~31~~ 2019, in urban Beijing, China. To our best knowledge, it is the first time presenting a simultaneous measurement of HCl and HBr with high time-resolution in urban Beijing. Besides, we identify the potential source that contributed to the high levels of gaseous HCl and HBr during wintertime and early springtime. In addition, we estimate the contribution of gaseous HCl and HBr on the production rates of atomic Cl and Br in urban Beijing.

2. Methodology

2.1 Sampling site.

The field measurements were conducted at Beijing University of Chemical Technology (BUCT) monitoring station (39.94° N, 116.30° E), located in an urban area of Beijing, China (Figure 1) where the nearest coastline locates about 150 km away in the southeast. The sampling site is about 130 m north to the Zizhuyuan Road and 550 m west to the West Third Ring Road, which is one of the main roads in Beijing. Besides the effect of traffic, this site is also surrounded by local commercial properties and residential dwellings. Thus, the BUCT sampling site can be regarded as a typical urban site. More information about this sampling site can be found in previous studies (Cai et al., 2020;Kontkanen et al., 2020;Zhou et al., 2020;Chu et al., 2021). The instruments were deployed at the roof of a teaching building, which is approximately 15 m above the ground level.

2.2 CI-APi-LTOF mass spectrometer.

The working principle of CI-APi-LTOF (Aerodyne Research Inc. and Tofwerk AG) has been described elsewhere (Yao et al., 2020;Eisele and Tanner, 1993;Yao et al., 2018), therefore only details relevant to this present work were discussed. A typical mass spectrum during our field measurement was depicted in Figure S1. The dominant reagent ions were nitrate ions (NO_3^-, and $HNO_3 \cdot NO_3^-$) and nitrite ions (NO_2^-). Among them, nitrate ions were generated by exposure of sheath flow (pure air with RH ~5%) which carried gaseous HNO_3. Besides the nitrate ions that acted as dominate reagent ions, nitrite ions were formed from the reaction of a small amount of NO_2 (~1 ppb) in the sheath flow with O_2^- and OH^- which were generated from the exposure of sheath flow (pure air with RH ~5%) to an X-ray source (Hamamatsu L9491) (Figure S5) (Arnold et al., 1995;Skalny et al., 2004). Considering nitrate ions were still the dominant reagent ions (Figure S1), the CI-

APi-LTOF was actually operated as a typical nitrate-CI-APi-LTOF.

Ambient air was drawn into the CI-inlet through a 3 quarter-inch stainless steel tube with a flow of ~8 L min^{-1}. A small mixed flow (~0.8 L min^{-1} controlled by a critical orifice with 300 μm diameter) entered the APi-LTOF and be analyzed. The CI-APi-LTOF was operated in the negative V-mode with the mass resolving power of ~10000 Th/Th and the mass accuracy better than 5 ppm. Data of CI-APi-LTOF were acquired with 5 s time resolution, and the recorded data were further analyzed with a MATLAB tofTools package (Junninen et al., 2010).

2.3 Detection and quantification of HCl and HBr

From Table 1, the ~~Gas~~gas-phase acidity ($-\Delta G$) of HCl is 1354 kJ mol^{-1} which is larger than that of HNO_3 (1329 kJ mol^{-1}). Besides, the enthalpy (ΔH) of HNO_3 and Cl^- is 32.8 kcal mol^{-1}, which is higher than that of HCl and NO_3^- (22.9 kcal mol^{-1}) hinting that the reaction of HCl and NO_3^- was unlikely to occur (Figure S4a). Additionally, from a previous study, the reaction rate (< 10^{-12} molecules cm^{-3} s^{-1}) between NO_3^- and HCl was significantly less than that (1.4×10^{-9} molecules cm^{-3} s^{-1}) of NO_2^- with HCl (Ferguson et al., 1972). Therefore, the HCl is likely mainly charged by NO_2^- instead of NO_3^- to result in Cl^- formation. The ion-molecule reaction between nitrite ions and HCl can be written as follows (Ferguson et al., 1972):

$$NO_2^- + HCl \rightarrow Cl^- + HNO_2 \qquad (R6)$$

In addition to NO_2^-, the HCl can also react with O_2^-, leading to Cl^- and Br^- formation via reaction (R7).

$$O_2^- + HCl \rightarrow Cl^- + HO_2 \qquad (R7)$$

Therefore, HCl can be quantified according to:

$$[HCl] = C_{HCl} \times \frac{[Cl^-]}{(NO_2^- + O_2^-)} \qquad E\ (1)$$

where C_{HCl} (in units of molecules cm^{-3}) is a calibration coefficient of HCl. Based on ambient data, a very small fraction (less than 5%) of Cl^- (or HCl) would react with HNO_3 (or NO_3^-) in the sheath flow to form $Cl^-{\cdot}HNO_3$ (or $HCl{\cdot}NO_3^-$). Thus, the signals of $Cl^-{\cdot}HNO_3$ (or $HCl{\cdot}NO_3^-$) were not taken into account for HCl quantification. The background measurement was carried out by sampling zero air. From Figure S7, the background signals were significantly lower than that of ambient air and injected HCl and HBr. The limits of detection (LODs, 3σ) were 1×10^8 and 1×10^7 molecules cm^{-3} (i.e., 4 and 0.5 ppt) for HCl and HBr, respectively. ~~The normalized background signals of HCl and HBr were 7×10^{-5} and 1×10^{-5}, respectively. And limits of detection (LODs, 3σ), corresponding to 2 min background periods, were 1×10^8 and 1×10^7 molecules cm^{-3} (4 and 0.5 ppt) for HCl and HBr, respectively.~~ Using 4-days synchronous gaseous HCl concentrations measured by a Monitor for AeRosols and Gases in Ambient air (MARGA, Metrohm Inc., Switzerland), an indirect calibration was adopted to quantify the HCl measured by the CI-APi-LTOF (Section S5 in Supporting Information). The obtained calibration factor C_{HCl} for HCl is $3 \pm 0.1\times10^{12}$ molecules cm^{-3} (Figure S8b) and the uncertainty of ± 30% (Section S5) was applied to the reported HCl concentrations. Similar to HCl, the same uncertainty was also adopted for HBr mixing ratios. It should be noted that our assumptions lead towards a lower limit estimate of HCl and HBr concentrations, due to other potential uncertainties (e.g., different sensitivities of HCl and HBr) were not taken into account. ~~The obtained calibration factor C_{HCl} for HCl is $2.84\pm0.073\times10^{12}$ molecules cm^{-3} (Figure S8b).~~

On the basis of $-\Delta G$ of HBr, HNO_3, HNO_2 and HO_2 and the enthalpy (ΔH) calculations (Table 1, Figure 2 and S4), besides the reaction with NO_2^- and O_2^-, similar with HCl, some of HBr could also react with NO_3^- to form Br^- via the reaction (R8) (Ferguson et al., 1972).

$$NO_3^- + HBr \rightarrow X^- + HNO_3 \qquad (R8)$$

Hence, the HBr should be quantified according to:

$$[HBr] = C_{HBr} \times \frac{[Br^-]}{(NO_2^- + O_2^-) + (NO_3^-)} \qquad \text{E (2)}$$

where C_{HBr} (in units of molecules cm^{-3}) is a calibration coefficient of HBr. However, due to a direct calibration for HBr was not available, the calibration coefficient of HCl (C_{HCl}) was utilized to semi-quantify HBr based on the following equation:

$$[HBr] = C_{HCl} \times \frac{[Br^-]}{(NO_2^- + O_2^-)} \qquad \text{E (3)}$$

Since the enthalpies (ΔH) of $HBr{\cdot}NO_3^-$ formed by HBr with NO_3^- (27.3 kcal mol^{-1}) and Br^- with HNO_3 (27.9 kcal mol^{-1}) were very close to each other (Figure S4b), it was difficult to quantify the specific contribution to Br^- from the reaction of HBr with NO_3^-. Also, the ratios of $Br^-{\cdot}HNO_3$ (or $HBr{\cdot}NO_3^-$) to Br^- were less than 4%. Therefore, in the equation 3, the reaction pathway of HBr with NO_3^- was not considered. The presented HBr concentrations should be treated as semi-quantification ones and upper limit values.

To confirm these ion-molecule reactions, high concentrations (undetermined) of gaseous HCl and HBr were mixed with zero air generated from a zero-air generator (Aadco 737), and then measured by CI-APi-LTOF (Section S4). After the injection of HCl and HBr, the signals of Cl^-, Br^-, $Cl^-{\cdot}HNO_3$ (or $HCl{\cdot}NO_3^-$) and $Br^-{\cdot}HNO_3$ (or $HBr{\cdot}NO_3^-$) started to increase (Figure S7), confirming that the HCl and HBr can be detected as Cl^-, Br^-, $Cl^-{\cdot}HNO_3$ and $Br^-{\cdot}HNO_3$ by CI-APi-LTOF.

2.4 Other auxiliary measurements.

Gaseous HCN and HCNO also can be detected by O_2^- through the ion-molecule reactions as follows:

$$O_2^- + HCN \rightarrow CN^- + HO_2 \qquad \text{(R9)}$$

$$O_2^- + HCNO \rightarrow CNO^- + HO_2 \qquad \text{(R10)}$$

The $-\Delta G$ of HCN and HCNO are 1433 kJ mol^{-1} and 1415 kJ mol^{-1}, respectively, which are higher than that of NO_2^- (1393 kJ mol^{-1}) (Table 1), and lower than that of O_2^- (1450 kJ mol^{-1}). Therefore, HCN and HCNO are able to be charged by O_2^- (but not NO_2^-) via deprotonation reaction to lead to CN^- and CNO^- formation. In this study, direct calibrations for HCN and HCNO were not available. Instead, the normalized signals of CN^- and CNO^- by O_2^- were tentatively utilized to indicate the abundance and trend of HCN and HCNO.

The meteorological parameters, including temperature and UVB intensities, were recorded by a weather station (Vaisala Inc., Finland). NO_2 was measured with a THERMO 42i NO-NO_2-NO_X Analyzer (Thermal Environment Instruments ~~(TEI)~~ Inc. USA). The mass concentrations of particulate chlorine and black carbon (BC) in $PM_{2.5}$ were measured by a time-of-flight aerosol chemical speciation monitor (ToF-ACSM, Aerodyne Research Inc., USA) and an aethalometer (AE33, Magee Inc., USA), respectively (Section S1 in Supporting Information).

Meanwhile, we applied 24h air mass back trajectory and Potential Source Contribution Function (PSCF) analyses to help to elucidate the potential source regions (i.e., air masses) of high levels of HCl and HBr. The detailed descriptions of PSCF and air mass trajectory analysis were described in the SI (Section S6) and previous literature (Wang et al., (2014, 2019b)). It is noted that the lifetime of gaseous HCl and HBr could be shorter than the length of the air mass trajectories. These analyses mainly aimed to point out the source regions of pollutant air masses that brought high levels of Cl and Br rather than the real-time origins of air parcels.

3. Results and discussions

3.1 HCl and HBr measurement.

Figure 3 shows the time series of gaseous HCl and HBr, temperature (T), and ultraviolet radiation b (UVB, 280-315 nm) intensities for the entire measurement period in winter and early spring of 2019 (February to April). High concentrations of HCl and HBr were observed for the whole measurement period with a clear diurnal variation (Figure ~~3c~~3e). The mean concentrations of HCl and HBr are 1×10^9 molecules cm^{-3} (37 ppt) and 2×10^8 molecules cm^{-3} (7 ppt), respectively. The maximum concentrations reach up to 6×10^9 molecules cm^{-3} (222 ppt) for HCl, and 1×10^9 molecules cm^{-3} (37 ppt) for HBr during the daytime.~~37 2622137The mean concentrations of HCl and HBr are 1.3 ± 1.1×10⁹ molecules cm⁻³ (50 ppt) and 1.92 ± 1.5×10⁸ moleculemoleculess cm⁻³ (7 ppt), respectively. The maximum concentrations reach up to 5.96×10⁹ molecules cm⁻³ (219 ppt) for HCl, and 1.2×10⁹ molecules cm⁻³ (44 ppt) for HBr during the daytime.~~ The concentrations of HCl and HBr showed a similar change in atmospheric temperature and UVB. For the first period of measurement (from 1 to 15 February), HCl and HBr concentrations are lower when the atmospheric temperature is close to 0℃ and the UVB intensities are relatively low. Yet, for the later period of March, the HCl and HBr concentrations begin to increase along with the rising of temperature and UV. In late March, even with higher temperature, due to the less abundant of HNO_3 and particulate chloride, the HCl and HBr concentrations remain at a relatively low level (Figure 3).~~ along For the first period of measurement (from February 1 to February 15), HCl and HBr concentrations are lower when the atmospheric temperature is close to 0℃ and UVB intensities are relatively low, while the HCl and HBr concentrations seems to increase together with the rising of temperatureHCl and HBr concentrations begin to increase together with the rising of temperature and UVB during April 2019.~~

The diurnal cycles of HCl and HBr are depicted in Figure 4a and 4b, respectively. The HCl concentrations are typically higher than HBr by approximately an order of magnitude; nevertheless, the diel patterns showed by these two species are quite similar to each other. It is noticed that both HCl and HBr began to increase after sunrise, and relatively high concentration was observed during the daytime (8:00 to 17:00). From Figure 4d, it also can be found that elevated temperature and high abundance of HNO_3 which was indicated as $[NO_2]$*[OH] could intensify the HCl releases from particulate chloride in the daytime from 08:00 to 17:00. The OH radical concentrations were calculated using J_{NO2} and J_{O1D} (Section S8). This phenomenon is consistent with our observation results above where the increase of temperature and UVB could reinforce the formation of chemicals (e.g., HNO_3) that promote the gas-particle partitioning or directly increase gas-phase formation rate of HCl and HBr (Crisp et al., 2014; Riedel et al., 2012), thus further enhancing the HCl and HBr (Figure 3). Although there is no direct measurement of particulate bromide (Br), considering the similarity in diurnal patterns and good correlation (r = 0.70) between HBr and HCl (Figure 4c), and HBr tracking well with the temperature and $[NO_2]$*[OH] (see Figure 3), it is rational to suppose HBr also predominantly derived from gas-particle partitioning process. The contribution by the reaction of bromine atoms with hydrocarbons to form HBr is likely not the dominant pathway as bromine atom is less reactive to hydrocarbons compared to the chlorine atom, and most often reacts with ozone (Simpson et al., 2015).

Our observation of daily averaged mass concentrations of particulate chloride (Cl (p)) in $PM_{2.5}$ showed a similar trend with daily averaged mixing ratios of gaseous HCl (Figure 5a). The difference from the ratios of HCl(g) to Cl(p) in February and March is likely due to the higher temperature in March (Figure 3 and 5a). In contrast, the diurnal variations of HCl and particulate Cl showed the opposite trend at daytime from 08:00 to 17:00 (Figure 5b). The mole ratios of HCl(g) to Cl(p) ranged from <0.1 at nighttime and early morning to >0.3 in the afternoon (Figure 5b). The enhancement of HCl(g)/Cl(p) during the noontime is owing to the large increase of gaseous HCl. It also suggested that the higher temperature and stronger photochemical reactions during the daytime would strongly influence HCl releases from particulate chloride in Beijing,

which will be further discussed in the following discussions. During the period between the late afternoon and midnight, the increase of Cl(p) and HCl(g) could be explained by the higher nighttime emissions of residential combustions such as wood and coal burnings in Beijing (Hu et al., 2017;Sun et al., 2016) and high abundance of gaseous HNO_3 are attributed to efficient nocturnal N_2O_5 chemistry (Tham et al., 2018). ~~HCl releasesfromparticulate [TVJ2]~~ity in~~From Figure 4d, it also can be found that elevated temperature and high abundance of HNO_3 which was indicated as $[NO_2]$*[OH] could intensify the gas to particle partitioning of chloride in the daytime from 08:00 to 17:00 (Figure 4d). The OH radical concentrations were calculated using J_{NO2} and J_{O1D} (Section S8). This phenomenon is consistent with our observation results above where the increase of temperature and UVB could reinforce the formation of chemicals (e.g., HNO_3) that promote the gas aerosol partitioning or directly increase gas phase formation rate of HCl and HBr (Crisp et al., 2014;Riedel et al., 2012), thus further enhancing the HCl and HBr (Figure 3). Although there is no direct measurement of particulate bromide (Br), considering the similar diurnal patterns and good correlation (r = 0.70) between HBr and HCl (Figure 4c), and HBr tracking well with the temperature and NO_2*OH (see Figure 3), it is rational to suppose HBr also predominantly derived from gas aerosol partitioning process. The contribution by reaction of bromine atoms with hydrocarbons to form HBr is likely not the dominant pathway as bromine atom is less reactive to hydrocarbons compared to the chlorine atom, and, most often reacts with ozone (Simpson et al., 2015).~~

~~HCl releases from particulate [TVJ3] are efficient 2 [TVJ4] 5Our observation of daily averaged mass concentrations of particulate chloride (Cl (p)Cl) in $PM_{2.5}$ showed a similar trend with daily averaged gaseous HCl (Figure S9a5a). The difference from the ratios of HCl(g) to Cl(p) in February and March is likely due to the increasing temperature in March. In contrast, the diurnal variations of HCl and particulate Cl showed the opposite trend at daytime from 08:00 to 17:00 (Figure S9b5b). The mole ratios of HCl(g) to Cl(p) ranged from <0.1 at nighttime and early morning to >0.3 in the afternoon (Figure 5b). The enhancement of HCl(g)/Cl(p) is owing to the large increase of gaseous HCl during the noontime. It also suggested that the higher temperature and stronger photochemical reactions during the daytime would strongly influence the chloride gas to particle partitioning in Beijing, which will be further discussed in the following discussions. The increase of HCl(g) and Cl(p) around midnight could be explained by the higher nighttime emissions of residential combustions such as wood and coal burnings in Beijing (Hu et al., 2017;Sun et al., 2016). The ratios of gaseous HCl to particulate Cl ranged from ~ 0.1 at nighttime and early morning to ~ 0.3 around noontime (Figure S9c), implying that there is intense gas to particle partitioning during the daytime. It also can be found that elevated temperature and high abundance of HNO_3 could intensify the gas to particle partitioning in the daytime (Figure 4d). This is consistent with our observation above where the increase of temperature and UVB could reinforce the formation of chemicals (e.g., HNO_3) that promote the gas aerosol partitioning or directly increase gas phase formation rate of HCl and HBr (Crisp et al., 2014;Riedel et al., 2012), thus further enhancing the HCl and HBr. Although there is no direct measurement of particulate bromide (Br), considering the diurnal pattern of HBr and the good correlation (r = 0.70) between HBr and HCl (Figure 4c), it is rational to suppose HBr also derived from gas aerosol partitioning process.~~

These observations showed that there is an abundance of gaseous HCl and HBr in the polluted urban environment. To our best of knowledge, this is the first concurrent observation of gaseous HCl and HBr in a polluted inland urban atmosphere. Although it is well known that the HCl is abundant in the polluted coastal and inland regions ~~regions~~, previous studies show that the typical HCl mixing ratios over the continental urban areas are less than 1 ppb (Crisp et al., 2014;Faxon and Allen, 2013;Le Breton et al., 2018; McNamara et al. 2020), which are similar to our observations at Beijing. In contrast, the presence of gaseous HBr in the urban regions is unknown prior to our observation. The significant concentration of HBr in the urban

atmosphere of Beijing is even comparable to the simulated concentrations in the marine environment, where concentration up to 2 ppt was reported (Fernandez et al., 2014). These elevated HCl and HBr in the urban of Beijing may point to the existence of Cl and Br sources in this region.

3.2 Source identification.

The natural sources of atmospheric Cl and Br include sea salt spray, wildfires and volcano emissions, while the anthropogenic emissions include coal combustions, traffic emissions as well as other industries such as pesticides, battery industry and waste incinerations (Simpson et al., 2015). Comparing with the sources of particulate Cl and Br that are widely studied and identified in previous literature, the origins of gaseous HCl and HBr are much less studied, due to their much shorter lifetime in the troposphere (Simpson et al., 2015).

According to air mass analysis (24h back-trajectory) for HCl and HBr during February and March (Figure ~~5a~~ 6a and b), the potential source regions of the selected periods with high-level concentrations of HCl (above 75% percentile) were located in the south of North China Plain, such as the south of Hebei province where heavy residential coal, biomass burning and industries emissions occurred (Fu et al., 2018~~b~~). Those figures further suggested that the high concentrations of HCl seemed not to be strongly affected by marine regions during our sampling period. Instead, the good correlation (r = 0.67) between hourly particulate Cl and BC together with the similar trend between particulate Cl and HCl suggested that HCl is likely to have the same original sources with particulate Cl and black carbon (BC) in $PM_{2.5}$ rather than marine sources (Figure ~~S9a~~ 5a and Figure S10a). Hydrocyanic acid (HCN) and isocyanic acid (HCNO), which were typically regarded as tracers for burning emissions, especially biomass burning process (Vigouroux et al., 2012;Adachi et al., 2019;Leslie et al., 2019;Wren et al., 2018;Priestley et al., 2018). Although a recent study showed that HCNO came from both primary emissions and secondary formation in the scale of North China Plain (NCP) during the daytime (Wang et al., 2020), the high correlations between HCN and HCNO (daytime, 08:00-17:00, r = 0.94 and nighttime, 18:00-07:00, r = 0.96) indicated that in urban Beijing, HCN and HCNO are mainly from primary emission (Figure ~~6c~~7c) and can be regarded as the tracers of combustion emissions. Thus, high correlations of measured gaseous HCl with HCN (r = 0.83) and HCNO (r = 0.90) further suggested that the HCl during our sampling period was more likely coming from combustion origins rather than marine source in the urban Beijing (Figure ~~6a~~ 7a and b). Since gaseous HCl could be affected by both emissions and gas/particle partitioning (shown in Figure 4d), we compared the daily concentrations of gaseous HCl and particulate Cl to minimize the influence of temperature and partitioning. The daily averaged HCl concentration had a high correlation with daily averaged particulate Cl (r = 0.84 and 0.70 for winter and spring periods, respectively) and BC concentration (r = 0.82), which is consistent with previous studies that particulate Cl, coal combustion organic aerosol (CCOA) and BC were highly correlated and likely to be from the same source in winter of Beijing (Hu et al., 2017;Hu et al., 2016).

Similar to HCl, the potential source regions for high Br concentrations were also located in the inland, demonstrating marine sources might not be the dominant source for gaseous HBr in winter of Beijing (Figure 6~~5~~b). The ratio of particulate Br/Na from previous literature in Beijing was 0.04 (He et al., 2001), which was much higher than those from seawater (0.018) and crustal dust (0.0006 to 0.0008) but much closer to those of biomass burning aerosols (0.01 to 0.06) (Sander et al., 2003). As discussed before, the good correlation (r = 0.70) between gaseous HCl and HBr also implied that their similar origins. In our study, moderate correlation coefficients were also observed between gaseous HBr and combustion tracers such as HCN, HCNO (0.63 and 0.62, respectively) and daily BC (r = 0.60) (Figure ~~6a~~7a, ~~6b~~ 7b and S10b). Multiple gaseous organic and inorganic Br compounds such as CH_3Br, Br_2, $BrNO_2$, BrCl, CH_3Br and CH_2Br_2 were also observed in different combustion processes such as biomass burning, coal combustions and waste

incineration in previous studies, further supporting the possibilities of combustion origins of the gaseous HBr in this study (Lee et al., 2018;Keene et al., 1999;Manö and Andreae, 1994). A recent airborne observation conducted in the U.S. found that high levels of reactive inorganic Br species in the plume from a coal power plant, likely due to the application of calcium bromide as additives in coal fuel (Lee et al., 2018). Together all these, in urban Beijing, the measured HBr was more likely coming from combustion sources such as biomass burning and coal combustion in the south of Beijing rather than marine sources. It is also interesting to note that in a previous marine study conducted at Oahu, Hawaii, gaseous Br was found to be 4 to 10 times higher than particulate Br (Moyers and Duce, 1972). On the other hand, from a previous observation conducted in urban Beijing, high levels of both gaseous (7 ng m^{-3}) and particulate (in total suspended particles (TSP), 18 ng m^{-3}) bromine were measured by offline sampling-organic solvent extraction and Instrumental Neutron Activation Analysis (INAA) method (Tian et al., 2005). ~~It is also interesting to note that in a previous marine study conducted at Oahu, Hawaii, gaseous Br was found to be 4 to 10 times higher than particulate Br (Moyers and Duce, 1972). On the other hand, from a previous observation conducted in urban Beijing, high levels of both gaseous (7 ng m^{-3}) and particulate (in total suspended particles (TSP), 18 ng m^{-3}) bromine were measured by offline sampling-organic solvent extraction and Instrumental Neutron Activation Analysis (INAA) method (Tian et al., 2005). , gaseous organic bromine was around 7 ng m^{-3} in Beijing, of which 6 ng m^{-3} was extractable and able to release to the atmosphere (Tian et al., 2005).~~ Considering the high concentration and reactivity of Br, gaseous Br from anthropogenic sources may play a more critical role in the urban atmosphere.~~Considering the high concentration and reactivity of both organic/inorganic Br, gaseous Br from anthropogenic sources may play a more critical role in the urban atmosphere.~~

3.3 Halogen~~s~~ atom production~~s~~.

To investigate the potential atmospheric implications of HCl and HBr on atmospheric oxidation capacity, we calculated the production rate of atomic Cl (P_{Cl}.) and Br (P_{Br}.) via the reactions of HCl and HBr with OH radicals. Figure ~~8~~7 shows the time series of P_{Cl}., P_{Br}., and the estimated diel concentration of OH calculated from photolysis rate (J_{O1D} and J_{NO_2}) and NO_2 concentration (C_{NO_2}) (Section S8). Note that the estimated peak concentrations of OH radicals varied between ~~2.8~~3×10^5 to ~4~~.3~~×10^6 ~~molecule~~molecules cm^{-3} during noontime. The reaction of HCl with OH radicals lead to a daily mean Cl atom production rate of 3~~.0~~×10^3 ~~molecule~~molecules cm^{-3} s^{-1} (Figure ~~7b~~8c). These rates fall within the range of Cl atom production rates (~10^3 to 10^6 ~~molecule~~molecules~~s~~ cm^{-3} s^{-1}) reported in polluted environments (Crisp et al., 2014;Hoffmann et al., 2018;McNamara et al 2020). For the reaction of HBr with OH, it is estimated to produce a daily mean of 8~~.4~~×10^3 ~~molecule~~molecules~~s~~ cm^{-3} s^{-1} of Br atom (Figure ~~7b~~8c). This result shows that in addition to the Cl atom, Br atom could also be present in urban Beijing and may act as important as the Cl atom in term of reaction with OH, since the P_{Br}. is about 2-3 times faster than the P_{Cl}. (Figure 8c~~7b~~). The average HCl and HBr concentrations were observed to be higher during the polluted days (daily mean $PM_{2.5}$ ≥ 75 μg/m^3), which is about 2-3 times higher than the clean days (daily mean $PM_{2.5}$ < 75 μg/m^3), as shown in Figure 8b. Consequently, the radical production rate also showed a difference between clean and polluted days (Figure 8d). The daily mean values~~s~~ of P_{Cl}. (up to 8~~8~~×10^3 molecules cm^{-3} s^{-1}) and P_{Br}. (2~~2~~×10^4 molecules cm^{-3} s^{-1}) in polluted days were both higher than those~~ose~~ of clean days by up to 2 times. This hints that the roles of HCl and HBr may be more significant in polluted environments.~~The average HCl and HBr concentrations were observed to be higher during the polluted days (daily $PM_{2.5}$ > 75 μg/m^3), which is about 2-3 times higher than the clean days (daily $PM_{2.5}$ < 75 μg/m^3), as shown in Figure 8a and 8b. Consequently, the radical production rate also showed difference between clean and polluted days. Daily mean value of P_{Cl}. (up to 7.4×10^3 molecules cm^{-3} s^{-1}) and P_{Br}. (1.8×10^4 molecules cm^{-3} s^{-1}) in polluted days were both higher than that of clean days by up to 2 times. This hints that the roles of HCl and HBr may be more significant in~~

polluted environments. Recent studies in several polluted sites of China suggested that the photolysis of $ClNO_2$ and Cl_2 are the dominant daytime Cl atom sources leading to Cl atom production rate up to 8×10^6 molecules cm^{-3} s^{-1} (Tham et al., 2016;Liu et al., 2017;Xia et al., 2020), while our observation of Cl atom production rate from HCl + OH is about 2×10^3 molecules cm^{-3} s^{-1}. Despite the lower production rate, the reaction of HCl with OH may also act as important recycling of Cl atom, which ultimately enhanced the atmospheric oxidation capacity (Riedel et al.,2012).Recent studies in several polluted sites of China suggested that the photolysis of $ClNO_2$ and Cl_2 are the dominant daytime Cl atom sources, lead to Cl atom production rate up to 8×10^6 molecules cm^{-3} s^{-1} (Tham et al., 2016;Liu et al., 2017;Xia et al., 2020), while our observation of Cl atom production rate from HCl+OH is about 1×10^4 molecules cm^{-3} s^{-1}. Despite the lower production rate, the reaction of HCl with OH may also act as important recycling of Cl atom, which ultimately enhanced the atmospheric oxidation capacity (Riedel et al.,2012). Recent studies in several polluted sites of China suggested that the photolysis of $ClNO_2$ and Cl_2 are the dominant daytime Cl atom sources, while the reaction of HCl with OH may also act as important recycling of Cl atom, which ultimately enhanced the atmospheric oxidation capacity (Tham et al., 2016;Liu et al., 2017;Xia et al., 2020). In analogous to the chlorine chemistry, the reaction of HBr with OH could be a significant source of Br atom in the daytime although rapid photolysis of Br_2 and $BrNO_2$ is believed to be the major Br atom source in a polluted urban environment as ubiquitous bromine species (e.g. Br_2, BrCl and $BrNO_2$) have been previously observed in residential coal burning and coal-fired power plant plumes (Lee et al., 2018;Peng et al., 2021). rural homes coalIn analogous to the chlorine chemistry, the reaction of HBr with OH could contribute to the recycling of Br atom, on top of the significant production from rapid photolysis of Br_2 and $BrNO_2$, which are believed to be ubiquitous in a polluted urban environment since significant levels of Br_2, BrCl and $BrNO_2$ were measured in the coal-fired power plant plumes (Lee et al., 2018;Peng et al., 2021)In analogous to the chlorine chemistry, the reaction of HBr with OH could contribute to the recycling of Br atom, on top of the significant production from rapid photolysis of Br_2 and $BrNO_2$, which are likely ubiquitous in a polluted urban environment since high levels of Br_2 and $BrNO_2$ were measured in the coal-fired power plant plumes (Lee et al., 2018).

4. Conclusions

In conclusion, we present the first concurrent measurement of both gaseous HCl and HBr in urban Beijing, a megacity with strong anthropogenic emissions in the North China Plain. Our observation surprisingly shows significant concentrations of HBr in urban Beijing, together with the elevated levels of HCl, throughout the winter and spring during our sampling period. Gaseous HCl and HBr are most likely originated from anthropogenic emissions such as burning activities (e.g., biomass burning and fossil fuel combustion) in the inland region rather than marine sources. Besides, the gas-particleaerosol partitioning may play a crucial role in contributing to elevated levels of HCl and HBr in urban Beijing. In polluted days, the concentrations of HCl and HBr are higher than those on clean days. These abundant HCl and HBr in the polluted urban troposphere may further influence the photochemistry of the atmosphere through the following two aspects: (1) direct contributions to the production of highly reactive halogen atom (e.g., Cl· and Br·), which can rapidly oxidize VOCs (reaction (R5)); (2) replenishing the halide ion (Cl^- and Br^-) in the aerosols for supporting the nocturnal heterogeneous production of $ClNO_2$ and $BrNO_2$, major sources of highly reactive halogen atom at sunrise (reaction (R3) and (R4)). Our observation of elevated HCl and HBr may indicate an important recycling pathway of Cl and Br species, and may provide a plausible explanation to the recent observations of widespread halogen activation in polluted areas of China (e.g. Tham et al., 2016;Zhou et al., 2018;Xia et al., 2020;Peng et al., 2020; Peng et al., 2021), which could have a significant influence on the atmospheric oxidation capacity and secondary aerosol formation. The atomic Cl and Br in polluted days might contribute higher to oxidation capacity than those on clean days. Furthermore, the additional insight on the HBr levels

at Beijing shows that the bromine chemistry, a previously neglected chemistry, may be important in inland megacities of China. Our results also suggest that understanding of gaseous HCl and HBr would be of much importance to the photochemistry studies as well as air quality improvement in urban areas of China.

Author Contributions

LY and YJT designed the research. XF, LY, YJT, JC, CY, YG, CL, KRD, FZ, ZL, BC, YM, LD, WD, JK, JTK, JZ, QZ, TK, SI, TP, DRW, VMK, YL, FB and MK carried out the observation, analyzed the data and interpreted the results. SI and TK provided quantum calculation results. XF, LY, YJT, and JC prepared the manuscript with contributions from all co-authors.

Declaration of competing interest

The authors declare that they have no known competing financial interests.

Acknowledgement

The work is supported by Academy of Finland (Center of Excellence in Atmospheric Sciences, project no. 307331, and PROFI3 funding, 311932), the European Research Council via ATM-GTP (742206) and the EMME-CARE project which has received funding from the European Union's Horizon 2020 Research and Innovation.

References:

Adachi, K., Sedlacek, A. J., Kleinman, L., Springston, S. R., and Buseck, P. R.: Spherical tarball particles form through rapid chemical and physical changes of organic matter in biomass-burning smoke, Proceedings of the National Academy of Sciences, 116, 201900129, 2019.

Arnold, S., Morris, R., Viggiano, A., and Jayne, J.: Ion chemistry relevant for chemical ionization detection of SO_3, J. Geophys. Res-Atmos.,, 100, 14141-14146, 10.1029/95JD01004, 1995.

Artiglia, L., Edebeli, J., Orlando, F., Chen, S., Lee, M.-T., Corral Arroyo, P., Gilgen, A., Bartels-Rausch, T., Kleibert, A., Vazdar, M., Carignano, M. A., Francisco, J. S., Shepson, P. B., Gladich, I., and Ammann, M.: A surface-stabilized ozonide triggers bromide oxidation at the aqueous solution-vapour interface, Nat. Commun., 8, 700, 10.1038/s41467-017-00823-x, 2017

Atkinson, R., Baulch, D. L., Cox, R. A., Crowley, J. N., Hampson, R. F., Hynes, R. G., Jenkin, M. E., Rossi, M. J., and Troe, J.: Evaluated kinetic and photochemical data for atmospheric chemistry: Volume III – gas phase reactions of inorganic halogens, Atmos. Chem. Phys., 7, 981-1191, 10.5194/acp-7-981-2007, 2007.

Bannan, T. J., Khan, M. A. H., Le Breton, M., Priestley, M., Worrall, S. D., Bacak, A., Marsden, N. A., Lowe, D., Pitt, J., Allen, G., Topping, D., Coe, H., McFiggans, G., Shallcross, D. E., and Percival, C. J.: A Large Source of Atomic Chlorine From $ClNO_2$ Photolysis at a U.K. Landfill Site, Geophysical Research Letters, 46, 8508-8516, 10.1029/2019GL083764, 2019.

Bedjanian, Y., and Poulet, G.: Kinetics of halogen oxide radicals in the stratosphere, Chem. Rev., 103, 4639, 2003.

Brown, S. S., and Stutz, J.: Nighttime radical observations and chemistry, Chemical Society Reviews, 41, 6405-6447, 10.1039/C2CS35181A, 2012.

Cai, J., Wang, J., Zhang, Y., Tian, H., Zhu, C., Gross, D. S., Hu, M., Hao, J., He, K., and Wang, S.: Source apportionment of Pb-containing particles in Beijing during January 2013, Environmental Pollution, 2017.

Cai, J., Chu, B., Yao, L., Yan, C., Heikkinen, L. M., Zheng, F., Li, C., Fan, X., Zhang, S., Yang, D., Wang, Y., Kokkonen, T. V., Chan, T., Zhou, Y., Dada, L., Liu, Y., He, H., Paasonen, P., Kujansuu, J. T., Petäjä, T., Mohr, C., Kangasluoma, J., Bianchi, F., Sun, Y., Croteau, P. L., Worsnop, D. R., Kerminen, V.-M., Du, W., Kulmala, M., and Daellenbach, K. R.: Size-segregated particle number and mass concentrations from different emission sources in urban Beijing, Atmos. Chem. Phys., 20, 12721-12740, 10.5194/acp-20-12721-2020, 2020.

Calvert, J and Lindberg, S.: The potential influence of iodine-containing compounds on the chemistry of the troposphere in the polar spring. II. Mercury depletion. Atmospheric Environment 38(30), 5105-5116, 2004.

Chen, D., Huey, L. G., Tanner, D. J., Salawitch, R. J., Anderson, D. C., Wales, P. A., Pan, L. L., Atlas, E. L., Hornbrook, R. S., Apel, E. C., Blake, N. J., Campos, T. L., Donets, V., Flocke, F. M., Hall, S. R., Hanisco, T. F., Hills, A. J., Honomichl, S. B., Jensen, J. B., Kaser, L., Montzka, D. D., Nicely, J. M., Reeves, J. M., Riemer, D. D., Schauffler, S. M., Ullmann, K., Weinheimer, A. J., and Wolfe, G. M.: Airborne measurements of BrO and the sum of HOBr and Br_2 over the Tropical West Pacific from 1 to 15 km during the CONvective TRansport of Active Species in the Tropics (CONTRAST) experiment, J. Geophys. Res-Atmos., 121, 12,560-512,578, https://doi.org/10.1002/2016JD025561, 2016.

Chu, B. W., Dada, L., Liu, Y. C., Yao, L., Wang, Y. H., Du, W., Cai, J., Dallenbach, K. R., Chen, X. M., Simonen, P., Zhou, Y., Deng, C. J., Fu, Y. Y., Yin, R. J., Li, H. Y., He, X. C., Feng, Z. M., Yan, C., Kangasluoma, J., Bianchi, F., Jiang, J. K., Kujansuu, J., Kerminen, V. M., Petaja, T., He, H., and Kulmala,

M.: Particle growth with photochemical age from new particle formation to haze in the winter of Beijing, China, Sci. Total Environ., 753, 2021.

Crisp, T., Lerner, B., Williams, E., Quinn, P., Bates, T., and Bertram, T.: Observations of gas-phase hydrochloric acid in the polluted marine boundary layer, J. Geophys. Res-Atmos.,, 119, 6897-6915, 10.1002/2013JD020992, 2014.

Eisele, F. L., and Tanner, D. J.: Measurement of the Gas-Phase Concentration of H_2SO_4 and Methane Sulfonic-Acid and Estimates of H_2SO_4 Production and Loss in the Atmosphere, J. Geophys. Res-Atmos., 98, 9001-9010, 1993.

Faxon, C. B., and Allen, D. T.: Chlorine chemistry in urban atmospheres: a review, Environmental Chemistry, 10, 221, 2013.

Ferguson, E. E., Dunkin, D. B., and Fehsenfeld, F. C.: Reactions of NO_2^- and NO_3^- with HCl and HBr, Journal of Chemical Physics, 57, 1459-1463, 1972.

Fernandez, R. P., Salawitch, R. J., Kinnison, D. E., Lamarque, J. F., and Saiz-Lopez, A.: Bromine partitioning in the tropical tropopause layer: implications for stratospheric injection, Atmos. Chem. Phys., 14, 17857-17905, 2014.

Finlayson-Pitts, B. J., Ezell, M. J., and Pitts, J. N.: Formation of chemically active chlorine compounds by reactions of atmospheric NaCl particles with gaseous N_2O_5 and $ClONO_2$, Nature, 337, 241-244, 10.1038/337241a0, 1989.

~~Fu, X., Wang, T., Wang, S., Zhang, L., Cai, S., Xing, J., and Hao, J.: Anthropogenic Emissions of Hydrogen Chloride and Fine Particulate Chloride in China, Environ. Sci. Technol., 52, 1644-1654, 10.1021/acs.est.7b05030, 2018a.~~

Fu, X., Wang, T., Wang, S., Zhang, L., Cai, S., Xing, J., and Hao, J.: Anthropogenic Emissions of Hydrogen Chloride and Fine Particulate Chloride in China, Environ. Sci. Technol., 52, 1644-1654, 2018~~b~~.

Gard, E. E., Kleeman, M. J., Gross, D. S., Hughes, L. S., Allen, J. O., Morrical, B. D., Fergenson, D. P., Dienes, T., E. Gälli, M., Johnson, R. J., Cass, G. R., and Prather, K. A.: Direct Observation of Heterogeneous Chemistry in the Atmosphere, Science, 279, 1184, 10.1126/science.279.5354.1184, 1998.

Glasow, R. V., and Crutzen, P. J.: Tropospheric Halogen Chemistry, Treatise on Geochemistry, 5, 19-69, 2014.

Graedel, T. E., and Keene, W. C.: Tropospheric budget of reactive chlorine, Global Biogeochemical Cycles, 9, 47-77, 1995.

Hara, H., Kato, T., and Matsushita, H.: The Mechanism of Seasonal Variation in the Size Distributions of Atmospheric Chloride and Nitrate Aerosol in Tokyo, Bulletin of the Chemical Society of Japan, 62, 2643-2649, 10.1246/bcsj.62.2643, 1989.

Haskins, J. D., Jaeglé, L., Shah, V., Lee, B. H., Lopez-Hilfiker, F. D., Campuzano-Jost, P., Schroder, J. C., Day, D. A., Guo, H., Sullivan, A. P., Weber, R., Dibb, J., Campos, T., Jimenez, J. L., Brown, S. S., and Thornton, J. A.: Wintertime Gas-Particle Partitioning and Speciation of Inorganic Chlorine in the Lower Troposphere Over the Northeast United States and Coastal Ocean, Journal of Geophysical Research: Atmospheres, 123, 12,897-812,916, 10.1029/2018JD028786, 2018.

He, K. B., Yang, F. M., Ma, Y. L., Zhang, Q., Yao, X. H., Chan, C. K., Cadle, S., Chan, T., and Mulawa, P.: The characteristics of $PM_{2.5}$ in Beijing, China, Atmospheric Environment, 35, 4959-4970, 10.1016/s1352-2310(01)00301-6, 2001.

Hoffmann, E., Tilgner, A., Wolke, R., and Herrmann, H.: Enhanced Chlorine and Bromine Atom Activation by Hydrolysis of Halogen Nitrates from Marine Aerosols at Polluted Coastal Areas, Environ. Sci. Technol., 53, 10.1021/acs.est.8b05165, 2018.

Hu, W., Hu, M., Hu, W., Jimenez, J., Yuan, B., Chen, W., Wang, M., Wu, Y., Chen, C., Wang, Z., Peng, J., Zeng, L., and Shao, M.: Chemical composition, sources, and aging process of submicron aerosols in

Beijing: Contrast between summer and winter, Journal of Geophysical Research: Atmospheres, 121, 1955-1977, 10.1002/2015JD024020, 2016.

Hu, W., Hu, M., Hu, W., Chen, C., Wu, Y., and Guo, S.: Seasonal variations in high time-resolved chemical compositions, sources and evolution of atmospheric submicron aerosols in the megacity Beijing, Atmospheric Chemistry and Physics, 9979-10000, 10.5194/acp-17-9979-2017, 2017.

Junninen, H., Ehn, M., Petaja, T., Luosujarvi, L., Kotiaho, T., Kostiainen, R., Rohner, U., Gonin, M., Fuhrer, K., Kulmala, M., and Worsnop, D. R.: A high-resolution mass spectrometer to measure atmospheric ion composition, Atmos. Meas. Tech., 3, 1039-1053, 2010.

Keene, W. C., Khalil, M. A. K., Erickson, D. J., McCulloch, A., Graedel, T. E., Lobert, J. M., Aucott, M. L., Gong, S. L., Harper, D. B., Kleiman, G., Midgley, P., Moore, R. M., Seuzaret, C., Sturges, W. T., Benkovitz, C. M., Koropalov, V., Barrie, L. A., and Li, Y. F.: Composite global emissions of reactive chlorine from anthropogenic and natural sources: Reactive Chlorine Emissions Inventory, Journal of Geophysical Research: Atmospheres, 104, 8429-8440, 10.1029/1998jd100084, 1999.

Kontkanen, J., Deng, C., Fu, Y., Dada, L., Zhou, Y., Cai, J., Daellenbach, K. R., Hakala, S., Kokkonen, T. V., Lin, Z., Liu, Y., Wang, Y., Yan, C., Petäjä, T., Jiang, J., Kulmala, M., and Paasonen, P.: Size-resolved particle number emissions in Beijing determined from measured particle size distributions, Atmos. Chem. Phys., 20, 11329-11348, 10.5194/acp-20-11329-2020, 2020.

Lammel, G., Röhrl, A., and Schreiber, H.: Atmospheric lead and bromine in Germany, Environmental Science and Pollution Research, 9, 397, 10.1007/BF02987589, 2002.

Le Breton, M., Hallquist, Å. M., Pathak, R. K., Simpson, D., Wang, Y., Johansson, J., Zheng, J., Yang, Y., Shang, D., and Wang, H.: Chlorine oxidation of VOCs at a semi-rural site in Beijing: Significant chlorine liberation from $ClNO_2$ and subsequent gas and particle phase Cl-VOC production, Atmos. Chem. Phys., 18, (17), 13013-13030, 2018.

Lee, B. H., Lopez-Hilfiker, F. D., Schroder, J. C., Campuzano-Jost, P., Jimenez, J. L., McDuffie, E. E., Fibiger, D. L., Veres, P. R., Brown, S. S., Campos, T. L., Weinheimer, A. J., Flocke, F. F., Norris, G., O'Mara, K., Green, J. R., Fiddler, M. N., Bililign, S., Shah, V., Jaegle, L., and Thornton, J. A.: Airborne Observations of Reactive Inorganic Chlorine and Bromine Species in the Exhaust of Coal-Fired Power Plants, J Geophys Res Atmos, 123, 11225-11237, 10.1029/2018JD029284, 2018.

Leslie, M. D., Ridoli, M., Murphy, J. G., and Borduas-Dedekind, N.: Isocyanic acid (HNCO) and its fate in the atmosphere: a review, Environmental ence: Processes & Impacts, 21, 2019.

Li, Q., Badia, A., Wang, T., Sarwar, G., Fu, X., Zhang, L., Zhang, Q., Fung, J., Cuevas, C. A., Wang, S., Zhou, B., and Saiz-Lopez, A.: Potential Effect of Halogens on Atmospheric Oxidation and Air Quality in China, Journal of Geophysical Research: Atmospheres, 125, e2019JD032058, 10.1029/2019JD032058, 2020.

Liu, X., Qu, H., Huey, L. G., Wang, Y., Sjostedt, S., Zeng, L., Lu, K., Wu, Y., Hu, M., Shao, M., Zhu, T., and Zhang, Y.: High Levels of Daytime Molecular Chlorine and Nitryl Chloride at a Rural Site on the North China Plain, Environ. Sci. Technol., 51, 9588-9595, 10.1021/acs.est.7b03039, 2017.

Manö, S., and Andreae, M. O.: Emission of Methyl Bromide from Biomass Burning, Science, 263, 1255-1257, 1994.

McNamara, S. M., Kolesar, K. R., Wang, S., Kirpes, R. M., May, N. W., Gunsch, M. J., Cook, R. D., Fuentes, J. D., Hornbrook, R. S., Apel, E. C., China, S., Laskin, A., and Pratt, K. A.: Observation of Road Salt Aerosol Driving Inland Wintertime Atmospheric Chlorine Chemistry, ACS Central Science, 6, 684-694, 10.1021/acscentsci.9b00994, 2020.

Mielke, L. H., Furgeson, A., and Osthoff, H. D.: Observation of $ClNO_2$ in a Mid-Continental Urban Environment, Environ. Sci. Technol., 45, 8889-8896, 10.1021/es201955u, 2011.

Moyers, J. L., and Duce, R. A.: Gaseous and particulate bromine in the marine atmosphere, Journal of

Geophysical Research, 77, 5330-5338, 10.1029/JC077i027p05330, 1972.

Nolt, I. G., Ade, P., Alboni, F., Carli, B., Carlotti, M., Cortesi, U., Epifani, M., Griffin, M. J., Hamilton, P. A., Lee, C., Lepri, G., Mencaraglia, F., Murray, A. G., Park, J. H., Park, K., Raspollini, P., Ridolfi, M., and Vanek, M. D.: Stratospheric HBr concentration profile obtained from far-infrared emission spectroscopy, Geophysical Research Letters, 24, 281-284, 10.1029/97GL00034, 1997.

Osthoff, H. D., Roberts, J. M., Ravishankara, A. R., Williams, E. J., Lerner, B. M., Sommariva, R., Bates, T. S., Coffman, D., Quinn, P. K., Dibb, J. E., Stark, H., Burkholder, J. B., Talukdar, R. K., Meagher, J., Fehsenfeld, F. C., and Brown, S. S.: High levels of nitryl chloride in the polluted subtropical marine boundary layer, Nature Geoscience, 1, 324-328, 10.1038/ngeo177, 2008.

Peng, X., Wang, W., Xia, M., Chen, H., Ravishankara, A. R., Li, Q., Saiz-Lopez, A., Liu, P., Zhang, F., Zhang, C., Xue, L., Wang, X., George, C., Wang, J., Mu, Y., Chen, J., and Wang, T.: An unexpected large continental source of reactive bromine and chlorine with significant impact on wintertime air quality, National Science Review, 10.1093/nsr/nwaa304, 2020

Phillips, G. J., Tang, M. J., Thieser, J., Brickwedde, B., Schuster, G., Bohn, B., Lelieveld, J., and Crowley, J. N.: Significant concentrations of nitryl chloride observed in rural continental Europe associated with the influence of sea salt chloride and anthropogenic emissions, Geophysical Research Letters, 39, 10.1029/2012GL051912, 2012.

Priestley, M., Breton, M., Bannan, T., Leather, K., Bacak, A., Reyes Villegas, E., Vocht, F., Shallcross, B., Brazier, T., Khan, A., Allan, J., Shallcross, D., Coe, H., and Percival, C.: Observations of Isocyanate, Amide, Nitrate, and Nitro Compounds From an Anthropogenic Biomass Burning Event Using a ToF-CIMS, Journal of Geophysical Research: Atmospheres, 10.1002/2017JD027316, 2018.

Riedel, T. P., Bertram, T. H., Crisp, T. A., Williams, E. J., Lerner, B. M., Vlasenko, A., Li, S.-M., Gilman, J., de Gouw, J., Bon, D. M., Wagner, N. L., Brown, S. S., and Thornton, J. A.: Nitryl Chloride and Molecular Chlorine in the Coastal Marine Boundary Layer, Environ. Sci. Technol., 46, 10463-10470, 10.1021/es204632r, 2012.

Riedel, T. P., Wagner, N. L., Dubé, W. P., Middlebrook, A. M., Young, C. J., Öztürk, F., Bahreini, R., VandenBoer, T. C., Wolfe, D. E., Williams, E. J., Roberts, J. M., Brown, S. S., and Thornton, J. A.: Chlorine activation within urban or power plant plumes: Vertically resolved $ClNO_2$ and Cl_2 measurements from a tall tower in a polluted continental setting, Journal of Geophysical Research: Atmospheres, 118, 8702-8715, 10.1002/jgrd.50637, 2013.

Roberts, T., Dayma, G., and Oppenheimer, C.: Reaction Rates Control High-Temperature Chemistry of Volcanic Gases in Air, Frontiers in Earth Science, 7, 154, 10.3389/feart.2019.00154, 2019.

Saiz-Lopez, A., Lamarque, J. F., Kinnison, D. E., Tilmes, S., Ordóñez, C., Orlando, J. J., Conley, A. J., Plane, J. M. C., Mahajan, A. S., Sousa Santos, G., Atlas, E. L., Blake, D. R., Sander, S. P., Schauffler, S., Thompson, A. M., and Brasseur, G.: Estimating the climate significance of halogen-driven ozone loss in the tropical marine troposphere, Atmos. Chem. Phys., 12, 3939-3949, 10.5194/acp-12-3939-2012, 2012.

Saiz-Lopez, A., and von Glasow, R.: Reactive halogen chemistry in the troposphere, Chem. Soc. Rev., 41, 6448-6472, 10.1039/c2cs35208g, 2012.

Sander, R., Keene, W. C., Pszenny, A. A. P., Arimoto, R., Ayers, G. P., Baboukas, E., Cainey, J. M., Crutzen, P. J., Duce, R. A., Hönninger, G., Huebert, B. J., Maenhaut, W., Mihalopoulos, N., Turekian, V. C., and Van Dingenen, R.: Inorganic bromine in the marine boundary layer: a critical review, Atmos. Chem. Phys., 3, 1301-1336, 10.5194/acp-3-1301-2003, 2003.

Sarwar, G., Simon, H., Xing, J., and Mathur, R.: Importance of tropospheric $ClNO_2$ chemistry across the Northern Hemisphere, Geophysical Research Letters, 41, 4050-4058, 10.1002/2014GL059962, 2014.

Sherwen, T., Evans, M. J., Sommariva, R., Hollis, L. D. J., Ball, S. M., Monks, P. S., Reed, C., Carpenter, L. J., Lee, J. D., Forster, G., Bandy, B., Reeves, C. E., and Bloss, W. J.: Effects of halogens on European air-quality, Faraday Discussions, 200, 75-100, 10.1039/C7FD00026J, 2017.

Simpson, W., Brown, S., Alfonso, S. L., Thornton, J., and Glasow, R.: Tropospheric Halogen Chemistry: Sources, Cycling, and Impacts, Chemical reviews, 115, 10.1021/cr5006638, 2015.

Skalny, J., Mikoviny, T., Matejcik, S., and Mason, N.: An analysis of mass spectrometric study of negative ions extracted from negative corona discharge in air, International Journal of Mass Spectrometry, 233, 317-324, 10.1016/j.ijms.2004.01.012, 2004.

Sun, Y., Du, W., Fu, P., Wang, Q., Li, J., Ge, X., Zhang, Q., Zhu, C., Ren, L., Xu, W., Zhao, J., Han, T., Worsnop, D. R., and Wang, Z.: Primary and secondary aerosols in Beijing in winter: sources, variations and processes, Atmospheric Chemistry and Physics, 16, 8309-8329, 10.5194/acp-16-8309-2016, 2016.

Tham, Y. J., Yan, C., Xue, L., Zha, Q., Wang, X., and Wang, T.: Presence of high nitryl chloride in Asian coastal environment and its impact on atmospheric photochemistry, Chinese Science Bulletin, 59, 356-359, 10.1007/s11434-013-0063-y, 2014.

Tham, Y. J., Wang, Z., Li, Q., Yun, H., Wang, W., Wang, X., Xue, L., Lu, K., Ma, N., Bohn, B., Li, X., Kecorius, S., Größ, J., Shao, M., Wiedensohler, A., Zhang, Y., and Wang, T.: Significant concentrations of nitryl chloride sustained in the morning: investigations of the causes and impacts on ozone production in a polluted region of northern China, Atmos. Chem. Phys., 16, 14959-14977, 10.5194/acp-16-14959-2016, 2016.

Tham, Y. J., Wang, Z., Li, Q., Wang, W., Wang, X., Lu, K., Ma, N., Yan, C., Kecorius, S., Wiedensohler, A., Zhang, Y., and Wang, T.: Heterogeneous N_2O_5 uptake coefficient and production yield of $ClNO_2$ in polluted northern China: roles of aerosol water content and chemical composition, Atmos. Chem. Phys., 18, 13155-13171, 10.5194/acp-18-13155-2018, 2018.

Thornton, J. A., Kercher, J. P., Riedel, T. P., Wagner, N. L., Cozic, J., Holloway, J. S., Dubé, W. P., Wolfe, G. M., Quinn, P. K., and Middlebrook, A. M.: A large atomic chlorine source inferred from mid-continental reactive nitrogen chemistry, Nature, 464, 271-274, 2010.

Tian, Q., Xu, D., Chai, Z., Lu, Y., and Xiong, Y.: Analysis on the organic bromine in the atmosphere in Beijing, Journal of Nuclear and Radiochemistry, 27, 236-238,252, 2005.

Vigouroux, C., Stavrakou, T., Whaley, C., Dils, B., Duflot, V., Hermans, C., Kumps, N., Metzger, J.-M., Scolas, F., Vanhaelewyn, G., Müller, J. F., Jones, D., Li, Q., and De Maziere, M.: FTIR time-series of biomass burning products (HCN, C_2H_6, C_2H_2, CH_3OH, and HCOOH) at Reunion Island (21°S, 55°E) and comparisons with model data, Atmos. Chem. Phys.,, 12, 13733-13786, 10.5194/acpd-12-13733-2012, 2012.

Wang, D. S., and Ruiz, L. H.: Secondary organic aerosol from chlorine-initiated oxidation of isoprene, Atmos. Chem. Phys., 17, 13491-13508, 10.5194/acp-17-13491-2017, 2017.

Wang, X., Jacob, D. J., Eastham, S. D., Sulprizio, M. P., Zhu, L., Chen, Q., Alexander, B., Sherwen, T., Evans, M. J., Lee, B. H., Haskins, J. D., Lopez-Hilfiker, F. D., Thornton, J. A., Huey, G. L., and Liao, H.: The role of chlorine in global tropospheric chemistry, Atmos. Chem. Phys., 19, 3981-4003, 10.5194/acp-19-3981-2019, 2019a.

Wang, Y. Q.: MeteoInfo: GIS software for meteorological data visualization and analysis, Meteorological Applications, 21, 2014.

Wang, Y. Q.: An Open Source Software Suite for Multi-Dimensional Meteorological Data Computation and Visualisation, Journal of Open Research Software, 7, 10.5334/jors.267, 2019b.

Wang, Z., Wang, W., Tham, Y. J., Li, Q., Wang, H., Wen, L., Wang, X., and Wang, T.: Fast heterogeneous N_2O_5 uptake and $ClNO_2$ production in power plant and industrial plumes observed in the nocturnal

residual layer over the North China Plain, Atmos. Chem. Phys., 17, 12361-12378, 10.5194/acp-17-12361-2017, 2017.

Wang, Z., Yuan, B., Ye, C., Roberts, J., Wisthaler, A., Lin, Y., Li, T., Wu, C., Peng, Y., Wang, C., Wang, S., Yang, S., Wang, B., Qi, J., Wang, C., Song, W., Hu, W., Wang, X., Xu, W., Ma, N., Kuang, Y., Tao, J., Zhang, Z., Su, H., Cheng, Y., Wang, X., and Shao, M.: High Concentrations of Atmospheric Isocyanic Acid (HNCO) Produced from Secondary Sources in China, Environmental Science & Technology, 10.1021/acs.est.0c02843, 2020.

Wren, S. N., John, L., Yuemei, H., Katherine, H., Gang, L., Mihele, C. M., Mittermeier, R. L., Craig, S., Wentzell, J. J. B., and Brook, J. R.: Elucidating real-world vehicle emission factors from mobile measurements over a large metropolitan region: a focus on isocyanic acid, hydrogen cyanide, and black carbon, Atmos. Chem. Phys., 18 (23), 16979-17001, 2018.

Xia, M., Peng, X., Wang, W., Yu, C., Sun, P., Li, Y., Liu, Y., Xu, Z., Wang, Z., Xu, Z., Nie, W., Ding, A., and Wang, T.: Significant production of $ClNO_2$ and possible source of Cl_2 from N_2O_5 uptake at a suburban site in eastern China, Atmos. Chem. Phys., 20, 6147-6158, 10.5194/acp-20-6147-2020, 2020.

Yang, X., Cox, R., Warwick, N., Pyle, J., Carver, G., O'Connor, F., and Savage, N.: Tropospheric bromine chemistry and its impacts on ozone: A model study, Journal of Geophysical Research, 110, 10.1029/2005JD006244, 2005.

Yang, X., Wang, T., Xia, M., Gao, X., Li, Q., Zhang, N., Gao, Y., Lee, S., Wang, X., Xue, L., Yang, L., and Wang, W.: Abundance and origin of fine particulate chloride in continental China, Science of The Total Environment, 624, 1041-1051, https://doi.org/10.1016/j.scitotenv.2017.12.205, 2018.

Yao, L., Garmash, O., Bianchi, F., Zheng, J., Yan, C., Kontkanen, J., Junninen, H., Mazon, S. B., Ehn, M., Paasonen, P., Sipila, M., Wang, M., Wang, X., Xiao, S., Chen, H., Lu, Y., Zhang, B., Wang, D., Fu, Q., Geng, F., Li, L., Wang, H., Qiao, L., Yang, X., Chen, J., Kerminen, V. M., Petaja, T., Worsnop, D. R., Kulmala, M., and Wang, L.: Atmospheric new particle formation from sulfuric acid and amines in a Chinese megacity, Science, 361, 278-281, 10.1126/science.aao4839, 2018.

Yao, L., Fan, X., Yan, C., Kurten, T., Daellenbach, K. R., Li, C., Wang, Y., Guo, Y., Dada, L., Rissanen, M. P., Cai, J., Tham, Y. J., Zha, Q., Zhang, S., Du, W., Yu, M., Zheng, F., Zhou, Y., Kontkanen, J., Chan, T., Shen, J., Kujansuu, J. T., Kangasluoma, J., Jiang, J., Wang, L., Worsnop, D. R., Petaja, T., Kerminen, V. M., Liu, Y., Chu, B., He, H., Kulmala, M., and Bianchi, F.: Unprecedented Ambient Sulfur Trioxide (SO_3) Detection: Possible Formation Mechanism and Atmospheric Implications, Environmental science & technology letters, 7, 809-818, 10.1021/acs.estlett.0c00615, 2020.

Zhou, W., Zhao, J., Ouyang, B., Mehra, A., Xu, W., Wang, Y., Bannan, T. J., Worrall, S. D., Priestley, M., Bacak, A., Chen, Q., Xie, C., Wang, Q., Wang, J., Du, W., Zhang, Y., Ge, X., Ye, P., Lee, J. D., Fu, P., Wang, Z., Worsnop, D., Jones, R., Percival, C. J., Coe, H., and Sun, Y.: Production of N_2O_5 and $ClNO_2$ in summer in urban Beijing, China, Atmos. Chem. Phys., 18, 11581-11597, 10.5194/acp-18-11581-2018, 2018.

Zhou, Y., Dada, L., Liu, Y., Fu, Y., Kangasluoma, J., Chan, T., Yan, C., Chu, B., Daellenbach, K. R., Bianchi, F., Kokkonen, T. V., Liu, Y., Kujansuu, J., Kerminen, V.-M., Petäjä, T., Wang, L., Jiang, J., and Kulmala, M.: Variation of size-segregated particle number concentrations in wintertime Beijing, Atmos. Chem. Phys., 20, 1201-1216, 10.5194/acp-20-1201-2020, 2020.

Table 1. Gas-phase acidities and deprotonated anion of a few compounds of interest.

Compounds	Formula	$-\Delta G^a$ (kJ mol^{-1})	Deprotonated Anion
Hydrobromic acid	HBr	1319	Br^-
Nitric acid	HNO_3	1329	NO_3^-
hydrochloric acid	HCl	1354	Cl^-
Nitrous Acid	HONO	1396	NO_2^-
Isocyanic Acid	HCNO	1415	CNO^-
Hydrocyanic Acid	HCN	1433	CN^-
Hydroperoxy radical	HO_2	1450	O_2^-
Hypobromous Acid	HOBr	1460	BrO^-
Hypochlorous Acid	HOCl	1461	ClO^-

[a] *Gas-phase acidity is defined as $-\Delta G$ for the protonation reaction ($H^+ + A^- \rightarrow HA$). Data are obtained from NIST Chemistry WebBook.*

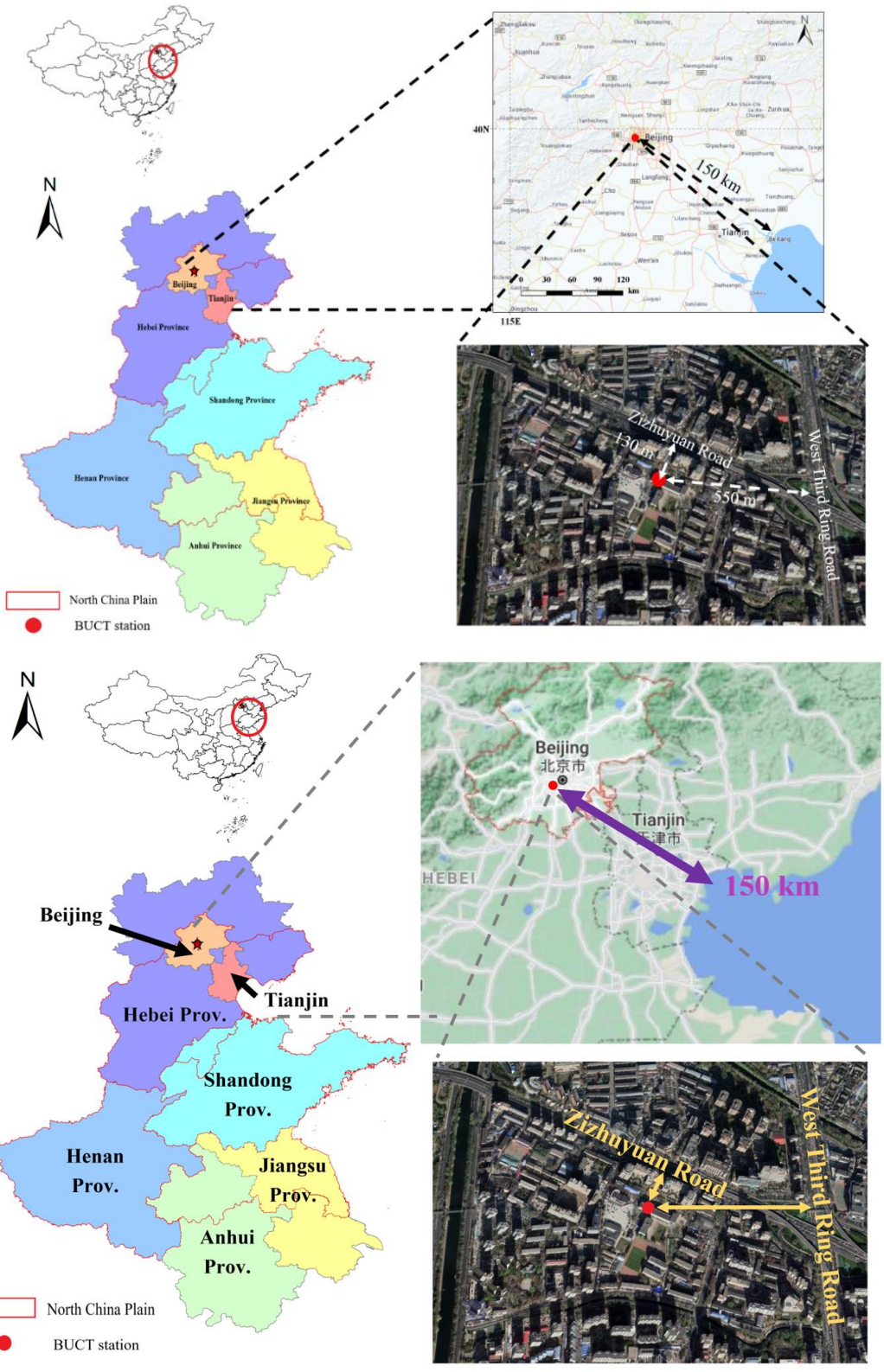

865

Figure 1. The location of BUCT measurement station. The satellite map was revised from ~~© Yahoo map and~~ © Google map.

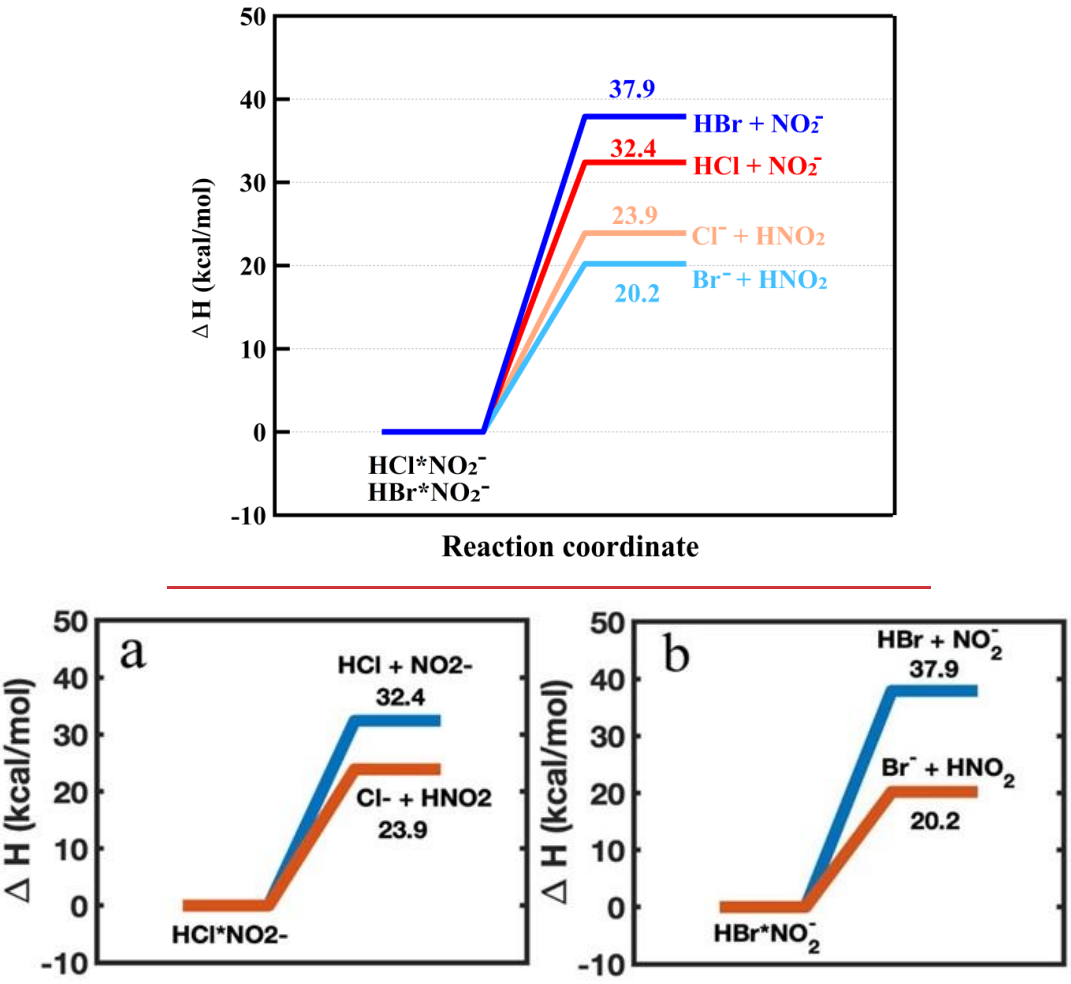

Figure 2. The calculated enthalpy of $HCl{\cdot}NO_2^-$ formed by HCl with NO_2^- and Cl^- with HNO_2 and enthalpy of $HBr{\cdot}NO_2^-$ formed by HBr with NO_2^- and Br^- with HNO_2 at the DLPNO-CCSD(T)/def2-QZVPP// ωB97X-D/aug-cc-pVTZ-PP level of theory.

~~**The enthalpy of $HCl{\cdot}NO_2^-$ formed by HCl with NO_2^- and Cl^- with HNO_2 (a) and the enthalpy of $HBr{\cdot}NO_2^-$ formed by HBr with NO_2^- and Br^- with HNO_2 (b) calculated at the DLPNO-CCSD(T)/def2-QZVPP// ωB97X-D/aug-cc-pVTZ-PP level of theory.**~~

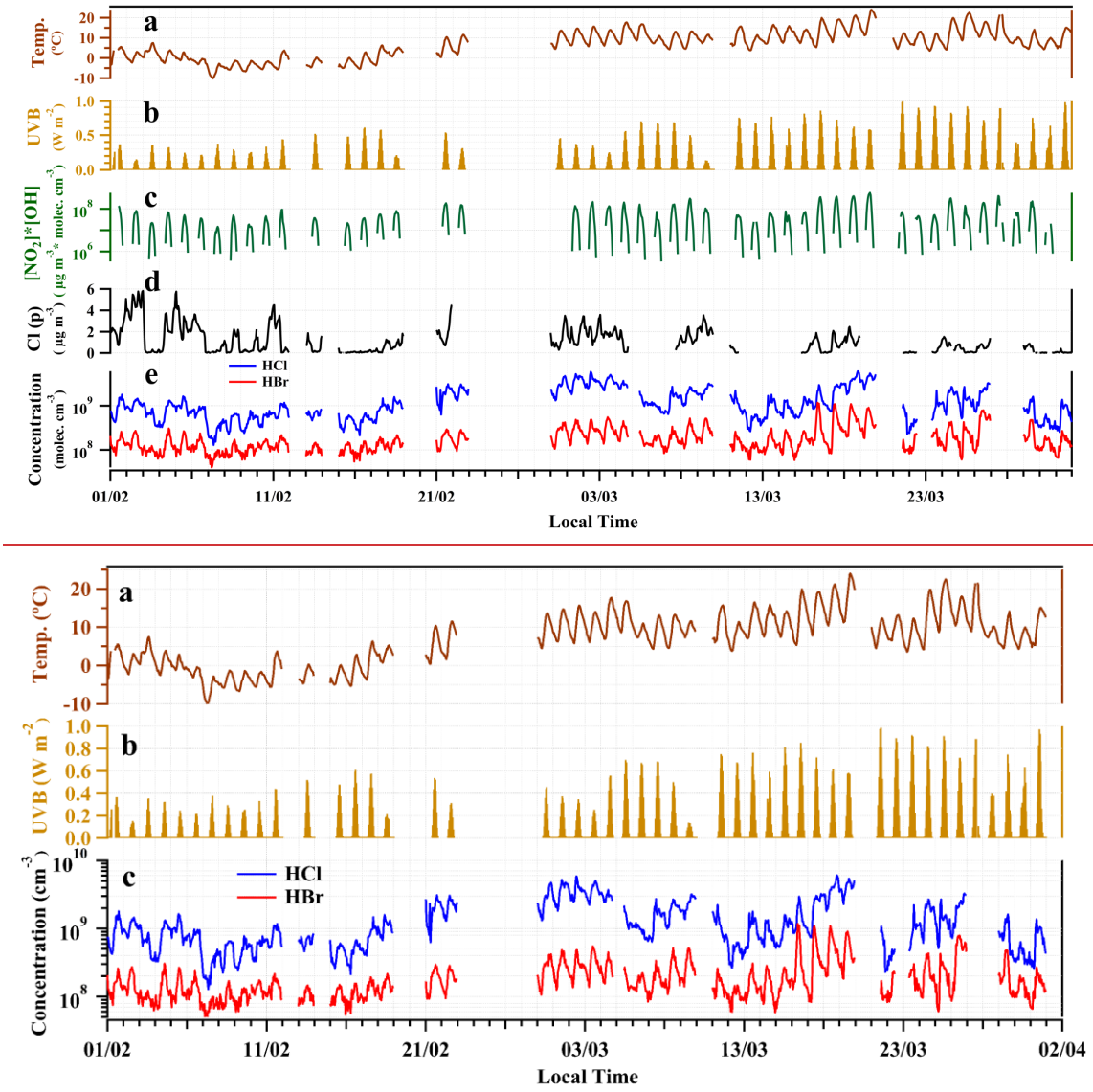

Figure 3. Time ~~series~~profiles of temperature (**a**), UVB intensities (**b**), [NO_2]*[OH] (**c**), particulate chloride (Cl-(p)) (**d**), and the mixing ratios of HCl and HBr (**e**). The data points are in hourly-average interval.

~~Time series of temperature (a), UVB (b) and concentrations of hydrochloric acid (HCl) and hydrobromic acid (HBr) measured by the CI-APi-LTOF (c). The data points are in hourly-average interval.~~

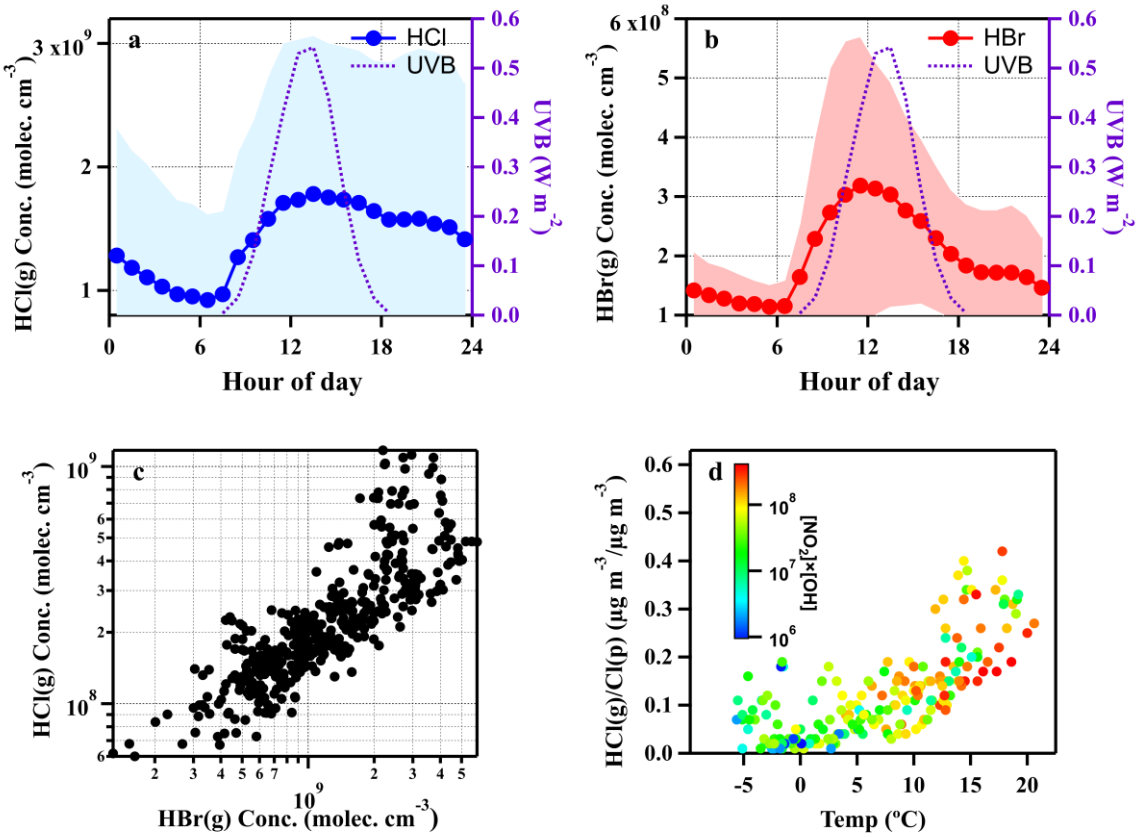
a
HCl
UVB
HCl(g) Conc. (molec. cm^{-3})
UVB (W m^{-2})
Hour of day
b
HBr
UVB
HBr(g) Conc. (molec. cm^{-3})
UVB (W m^{-2})
Hour of day
c
HCl(g) Conc. (molec. cm^{-3})
HBr(g) Conc. (molec. cm^{-3})
d
HCl(g)/Cl(p) (µg m^{-3}/µg m^{-3})
[NO$_2$]×[OH]
Temp (°C)

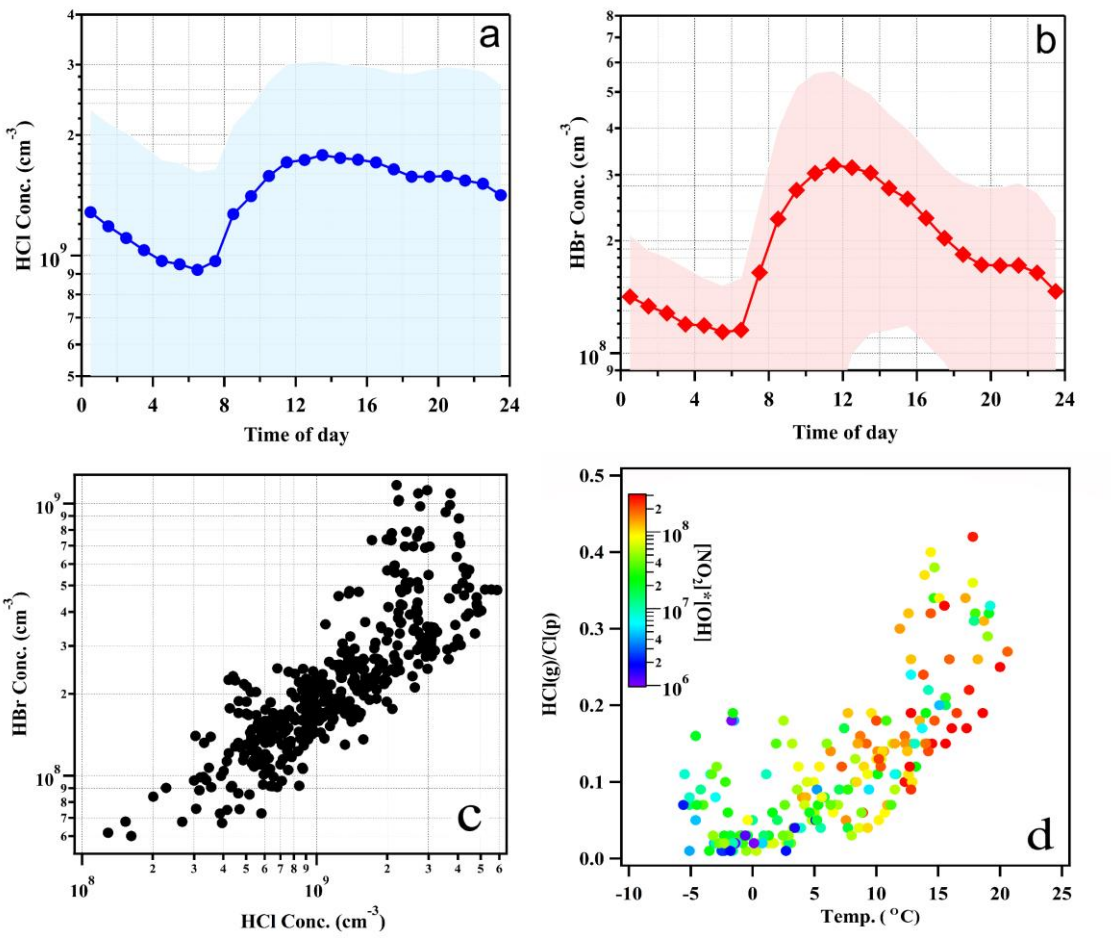

Figure 4. Diurnal variations of UVB intensities, HCl and HBr concentrations (averaged values ± one standard deviation) (**a** and **b**) and the correlation between HCl and HBr (**c**). In panel c, the data points are hourly averaged ones during daytime (8:00-17:00). Temperature dependence of gas to particle partitioning ratios of mass concentration of chloride, colour-coded by [NO_2]*[OH] which was indicated as the abundance of HNO_3 (**d**). All snowy and rainy days during the sampling period were excluded.

~~Diurnal variations of HCl and HBr concentrations (averaged values ± one standard deviation) (a and b) and the correlation between HCl and HBr (c). In panel c, the data points are daytime (8:00-17:00) hourly averaged ones. All snowy and rainy days were excluded. Temperature dependence of heterogeneous reaction in HCl, coloured by the abundance of HNO3 which was indicated by [NO2]*[OH] (d).~~

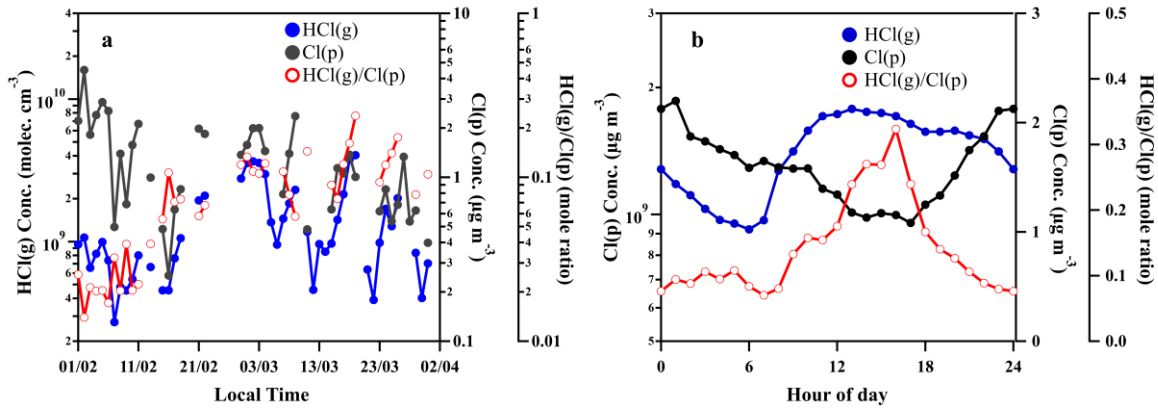

Figure 5. Time variation of daily averaged concentration of particulate chloride (Cl(p)) measured by ACSM, and gaseous HCl (HCl(g)) measured by CI-APi-LTOF and mole ratios of HCl(g)/Cl(p) (**a**) and diurnal variation of HCl(g), Cl (p) and mole ratios of HCl(g)/Cl(p) (**b**).

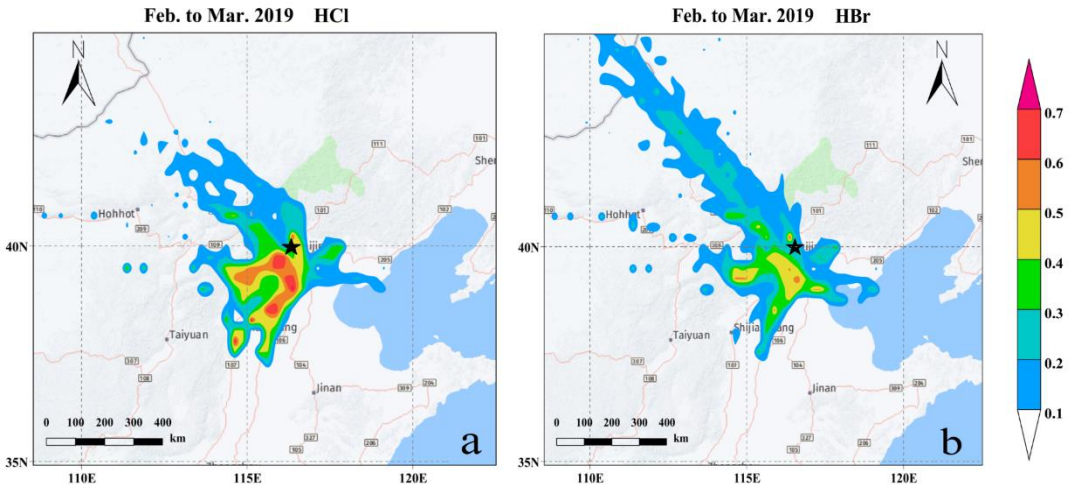

Figure ~~5~~6. The results of PSCF analysis for HCl (**a**) and HBr (**b**). Black stars mark the location of the sampling site.

~~**The 24h back trajectories of HCl (a) and HBr (b) concentration higher than 75% quantile at 100 m height in February and March using MeteoInfo PSCF modelling (Wang, 2014, 2019). The colour bar shows the weight among all backward trajectories arriving at BUCT, Beijing (marked as a black star).**~~

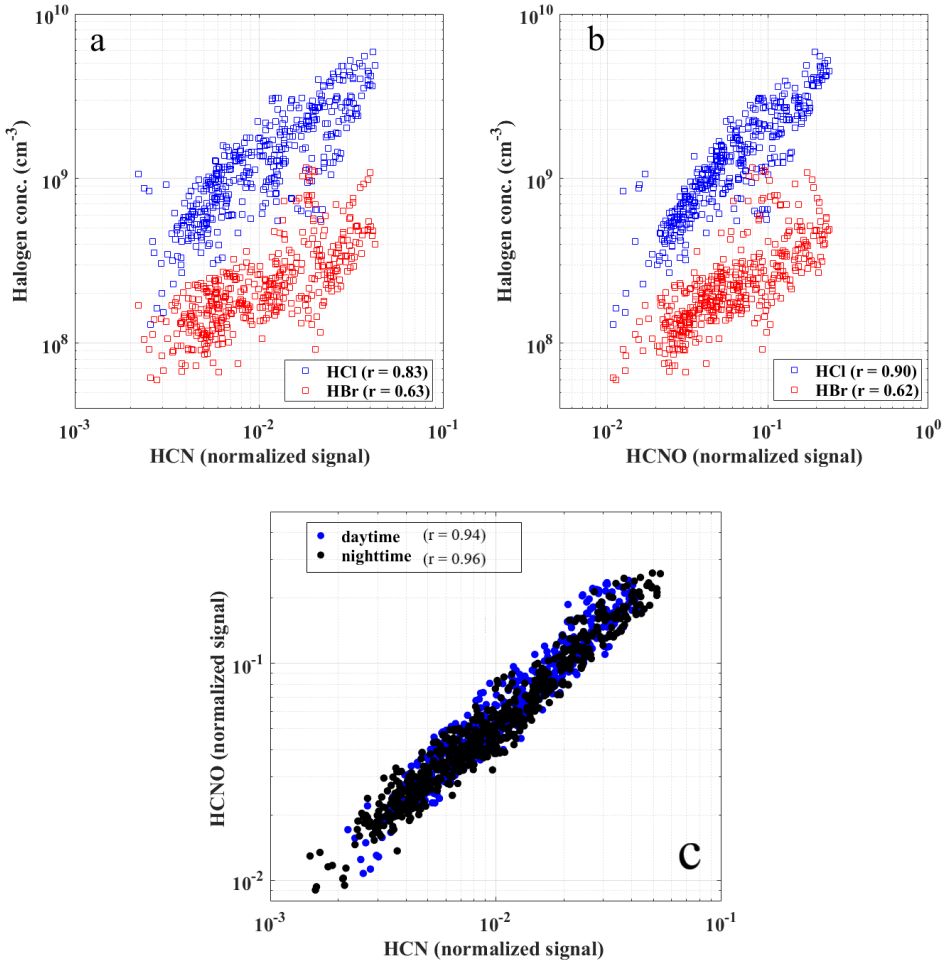
a
b
c
Halogen conc. (cm^{-3})
HCN (normalized signal)
HCNO (normalized signal)
HCl (r = 0.83)
HBr (r = 0.63)
HCl (r = 0.90)
HBr (r = 0.62)
daytime (r = 0.94)
nighttime (r = 0.96)

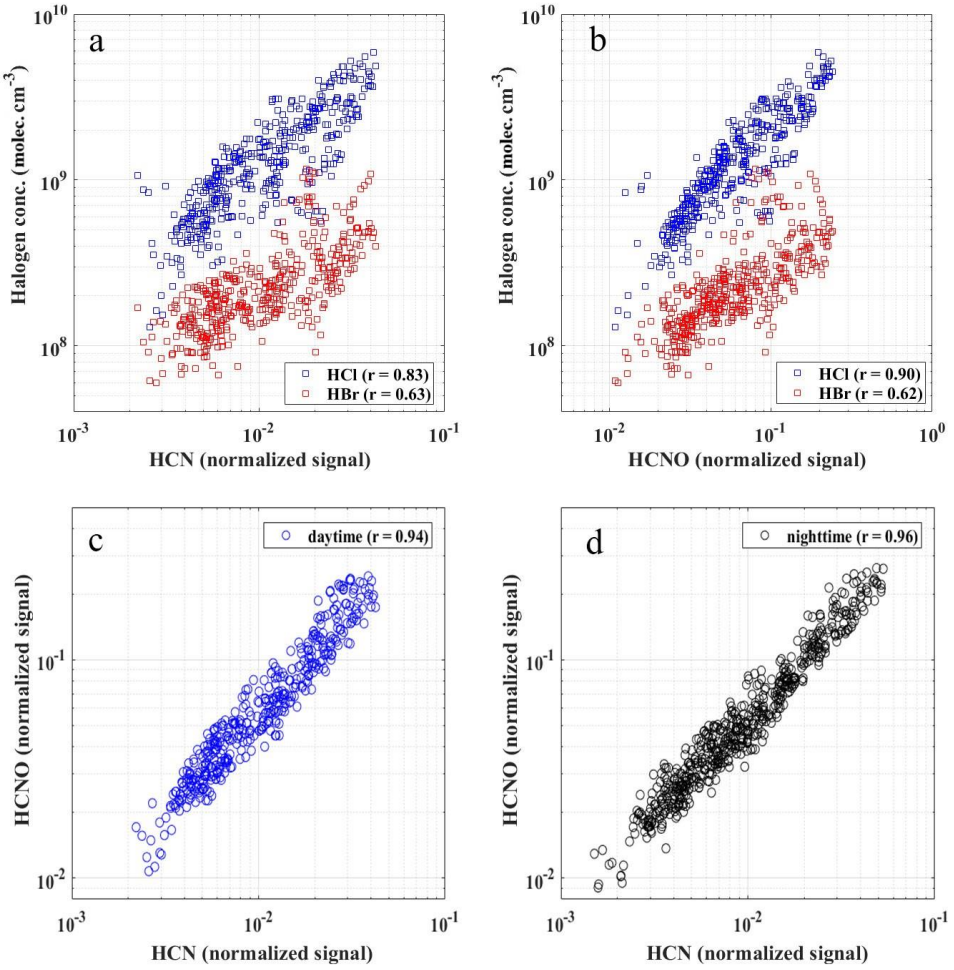

Figure ~~6~~7. The relationship of HCl and HBr concentrations with HCN ~~(a)~~ and HCNO ~~(b)~~ during the daytime (08:00-17:00) (**a** and **b**) and the correlations between HCN and HCNO during both daytime (08:00-17:00) (**c**) and nighttime (18:00-07:00 the next day) (**d**).

~~The relationship of HCl and HBr concentrations with HCN (a) and HCNO (b) during the daytime and the correlations between HCN and HCNO during both daytime (08:00-17:00) and nighttime (18:00-07:00 the next day) (c).~~

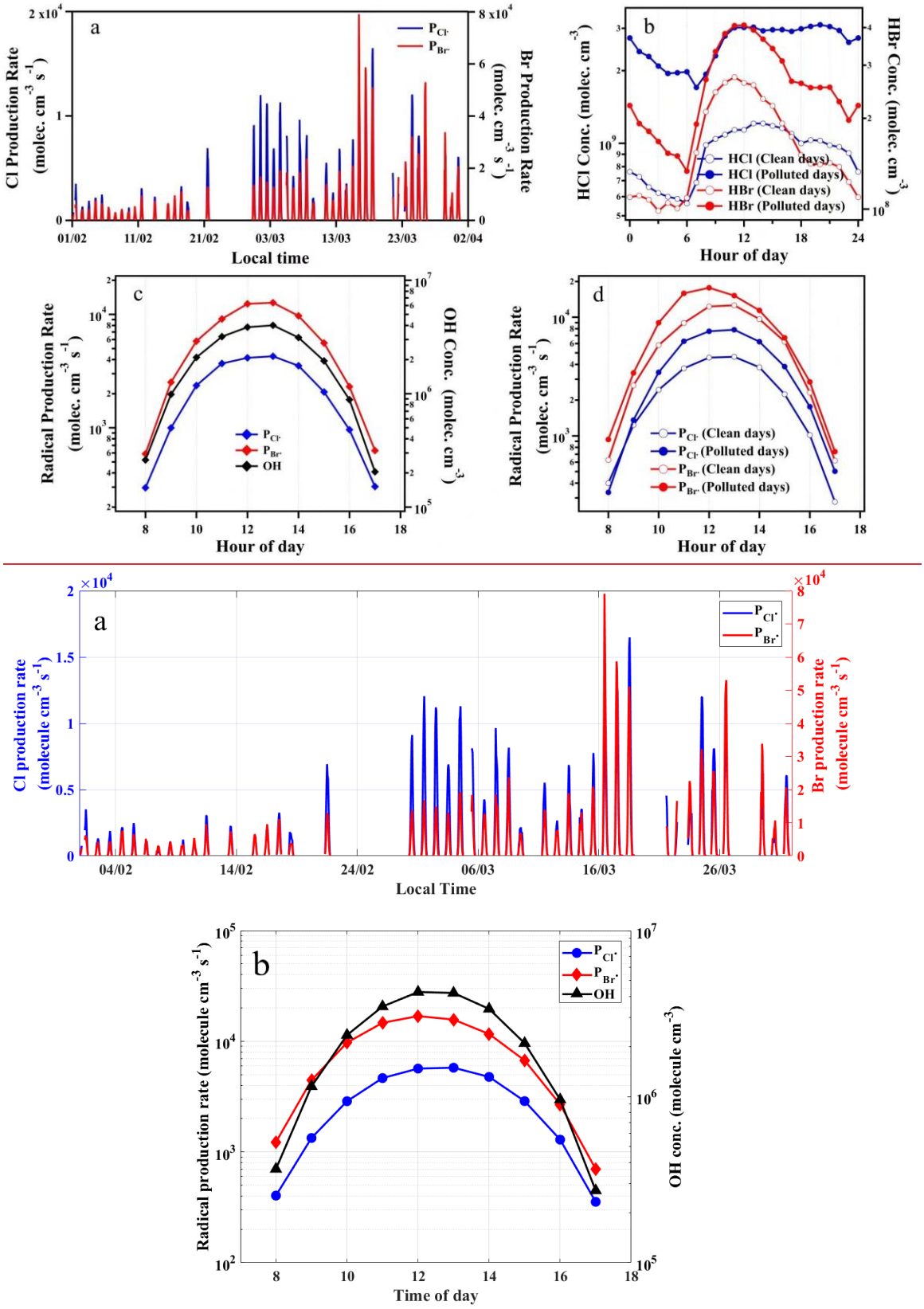

975 **Figure ~~7~~8.** Time series of calculated production rates of Cl and Br radicals during the observation period (**a**);

diurnal variations of HCl and HBr concentrations in clean and polluted days (**b**); diurnal variations of production rates of Cl and Br radicals, together with calculated OH radical concentrations (**c**) and production rates of Cl and Br radicals in clean and polluted days (**d**). The clean and polluted days were classified as daily $PM_{2.5}$ < 75 μg/m^3 and $PM_{2.5}$ ⩾ 75 μg/m^3, respectively. The data points are in the hourly-average interval and measured during observation periods from 1 February to 31 March 2019.~~Time series of production rates of Cl and Br radical were calculated based on IUPAC Task Group on Atmospheric Chemical Kinetic Data Evaluation (http://iupac.pole-ether.fr) during the observation period (**a**); diurnal variations of Diurnal variations of production rates of Cl and Br radical, calculated OH radical concentrations (**b**), HCl and HBr concentration in clean and polluted days (**c**) dtogether with and production rates of Cl and Br radical in clean and polluted days (**d**). The clean and polluted days were classified as daily $PM_{2.5}$ < 75 μg/m^3 and $PM_{2.5}$ 75 μg/m^3, respectively. The data points are in hourly-average interval and measured during observation periods from 1 February to 31 March, 2019.Time series (a) and diurnal pattern (b) of HCl, HBr radical production rate and OH concentration during the observation period.~~